Synthesis and Bulk Assembly Behavior of Linear–Dendritic Rod Diblock Copolymers

CATHERINE M. B. SANTINI,[1] MARK A. JOHNSON,[2] JAMES Q. BOEDICKER,[2] T. ALAN HATTON,[2] PAULA T. HAMMOND[2]

[1]Department of Materials Science and Engineering, Massachusetts Institute of Technology, Cambridge, Massachusetts 02139

[2]Department of Chemical Engineering, Massachusetts Institute of Technology, Cambridge, Massachusetts 02139

Received 7 January 2004; accepted 26 February 2004
DOI: 10.1002/pola.20156
Published online in Wiley InterScience (www.interscience.wiley.com).

ABSTRACT: Dendritic rod structures can be formed via the branching of dendritic elements from a primary polymer backbone; such systems present an opportunity to create nanoscale material structures with highly functional exterior regions. In this work, we report for the first time the synthesis of a hybrid diblock copolymer possessing a linear–dendritic rod architecture. These block copolymers consist of a linear poly(ethylene oxide)–poly(ethylene imine) diblock copolymer around which poly(amido amine) branches have been divergently synthesized from the poly(ethylene imine) block. The dendritic branches are terminated with amine or ester groups for the full generations and half-generations, respectively; however, the methyl ester terminal groups can also be readily converted into alkyl groups of various lengths, and this allows us to tune the hydrophilic/hydrophobic nature of the dendritic block and, therefore, the amphiphilic properties of the diblock copolymer and its tendencies toward microphase separation. The block copolymers exhibit semicrystallinity due to the presence of the poly(ethylene oxide) block; however, as the polymer fraction consisting of poly(ethylene oxide) decreases, the overall crystallinity also decreases, and it approaches zero at generation 2.0 and higher. The unfunctionalized block copolymers show weak phase segregation in transmission electron microscopy and differential scanning calorimetry at all generations. The addition of *n*-alkyl chains increases phase segregation, particularly at high alkyl lengths. The generation 3.5 polymer with *n*-dodecyl alkyl substitution has a rodlike or wormlike morphology consisting of domains of 4.1 nm, equivalent to the estimated cross section of the individual polymer chains. In this case, the nanometer scale of the polymer chains can be directly observed with transmission electron microscopy. © 2004 Wiley Periodicals, Inc. J Polym Sci Part A: Polym Chem 42: 2784–2814, 2004

Keywords: dendrimers; dendritic rod polymers; linear–dendritic diblock copolymers; poly(amido amine)

INTRODUCTION

Because of their nanoscale size and specific shape, dendrimers have often been proposed as molecular objects. Unlike traditional polymers, the size and shape of which are highly dependent on the environment, dendritic systems possess sizes and shapes that are much more robust because of their congested, hyperbranched nature, which prevents large fluctuations in these parameters. In addition, the dimensions of dendrimers can be tuned with the generation number, the size of the core, and the chemistry of the dendritic branches.

Correspondence to: P. T. Hammond (E-mail: hammond@mit.edu)

The shape most commonly associated with the term *dendrimer* is a sphere, consisting of three or four dendrons radiating out from a central small-molecule core. However, researchers have found it possible to alter the architecture of a dendrimer by modifying the number and position of the branch points in the core, resulting in the formation of new dendritic and hyperbranched architectures, by utilizing stable free-radical, anionic, and transition-metal-catalyst approaches to polymerization.[1–10] For example, rod-shaped dendrimers have been synthesized through the assembly of a dendron around each repeat unit of a linear polymer core,[11–20] either by the divergent addition of the branches to the linear polymer core or by the polymerization of a dendritic monomer. The steric hindrance imposed by the dendrons causes the polymer coil to unwind and behave as a rod, as verified by atomic force microscopy and transmission electron microscopy (TEM). Similarly, hybrid linear–dendritic diblock copolymers have been synthesized through the attachment of a single dendron to the end-functional group of a linear polymer. This has been accomplished through the coupling of a preformed dendron to the end-functional group of a linear polymer, the divergent construction of the dendron from the end-functional group of the linear polymer, and the growth of a linear chain from an already formed dendron.[21–38] Amphiphilic hybrid linear–dendritic rod diblock copolymers have been found to assemble into complex micelles in solution and form Langmuir and Langmuir–Blodgett films on air–water interfaces and monolayers at surfaces.[25–27,37,39–41] Linear–dendritic block copolymers have been shown to adopt both weakly segregated and well-defined morphologies in the bulk, which depend on the generation number of the dendritic block; the unique asymmetric architecture of these block copolymers has led to significant shifts in the morphological phase diagrams for these materials, as observed in systems with amorphous and crystallizable linear blocks.[25,26,34–36] The linear block in these hybrid systems provides a driving force by which order and assembly are induced via microphase segregation. This precise assembly and placement of the dendritic portion is another key factor in the preparation of molecular objects, providing another tool for the tuning of the molecular structure and function.

These block copolymer systems are examples of the use of unique macromolecular architectures to achieve a range of self-assembled structures in solution and solid states based on an interplay of energetic effects such as crystallization and mesomorphic ordering, copolymer asymmetry, and entropic effects that lead to a range of equilibrium structures. By combining two or more block segments with significantly different conformational or architectural arrangements, we can access new ordered morphologies. This has been demonstrated in the construction of linear rod-dendron block copolymers, which form bundled aggregates of predetermined size and order into smectic, cubic, and columnar discotic liquid-crystalline phases,[42–44] and in the synthesis of linear rod-linear coil block copolymers, which form thermotropic ordered phases consisting of aggregates.[45–47] A remarkable element of these block copolymers is the impact that the addition of even a relatively low-molar-mass element, such as a low-generation dendron or flexible-chain end group, can have on the final phase behavior. The balance between the preferred chain arrangements of two irregular blocks leads to the formation of nanoscale substructures, which can self-assemble into larger scale morphologies. The diverse range of available architectures allows the exploration of a variety of molecular objects derived from copolymer systems by increasing the number of molecular configurations and chain conformations achievable.

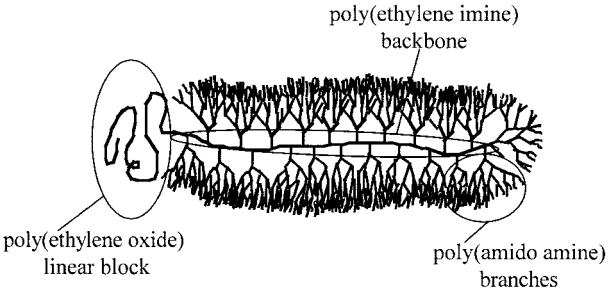

Figure 1. Graphical representation of the linear–dendritic rod diblock copolymers.

Here we introduce a new dendritic architecture, a linear–dendritic rod diblock copolymer, which is a combination of a hybrid linear–dendritic diblock copolymer and a dendritic rod. A graphical representation of this unique dendritic architecture is presented in Figure 1. This architecture is interesting because the polymer possesses not only a dendritic rod block but also a linear block that can act as a means of creating macromolecular amphiphiles with the ability to assemble at the air–water interface and the po-

tential for assembly in the bulk state via microphase segregation when the chemistry of the polymer is properly tuned. This system represents a new kind of asymmetric block copolymer that uses the conformational and size differences between a linear coil block and a more rigid and denser poly(amido amine) (PAMAM) rod block; these materials provide opportunities to explore nanostructured material assembly under these constraints in the bulk and solution states and to examine the impact of the dendritic rod system on phase morphologies. Potential future applications of this work are directed toward the development of ordered nanoporous assembled thin films for membrane separations and reactive membranes, templated molecular objects formed via intramolecular metal or metal oxide synthesis, and novel sensor and delivery vehicles. The use of a dendritic rod provides an extremely high surface functionality in the resulting polymer system, as well as a unique shape for the creation of ordered bicontinuous cylindrical or lamellar structures in thin films or at interfaces.

In this article, we report the synthesis of such a linear–dendritic rod diblock copolymer consisting of a poly(ethylene oxide)-linear poly(ethylene imine) (PEO–LPEI) diblock copolymer to which PAMAM branches have been divergently added around the poly(ethylene imine) (PEI) block. To make these diblock copolymers amphiphilic, we have functionalized the branch ends of the dendrimer with hydrophobic alkyl groups because both the poly(ethylene oxide) (PEO) and PAMAM dendritic blocks are naturally hydrophilic. Once the polymers were prepared and their chemical structure was confirmed, we examined the bulk thermal and morphological properties of these polymers with differential scanning calorimetry (DSC), small-angle X-ray scattering (SAXS), and transmission electron microscopy (TEM) to determine how these properties are affected by the generation number and end-group chemistry. In addition, by comparing the results for these linear–dendritic rod diblock copolymers with those from polymers possessing the same chemistry but different architectures, we have been able to determine how the architecture affects these parameters. The assembly behavior of these polymers in solution and at the air–water interface will be described in separate publications. In the remainder of this article, the synthesis and structural characterization of the linear–dendritic rod diblock copolymers are described, and the thermal and morphological properties of this interesting series of polymers and their self-assembly in the bulk state are discussed and compared with those of other chemically similar, but architecturally different, polymer systems. Simple changes in the dendritic end-group chemistry and dendrimer generation have been found to have a particularly large impact on the ordering, segregation, and phase behavior of these materials, as observed in other rod–coil polymers;[44–46,48,49] in this case, the weight fraction of the linear block varies greatly with the generation, and this amplifies the effects of dendron generation. Finally, the influence of substitution of the dendritic end groups of the comb copolymer block on ordering and morphology is addressed.

EXPERIMENTAL

Materials

Poly(ethylene glycol) monomethyl ether (molecular weight = 1900 g/mol) from Polysciences was purified twice by precipitation from chloroform into a 10-fold excess of ethyl ether. It was then dried on a vacuum line for 1 day and in a vacuum desiccator with P_2O_5 for an additional day. Tosyl chloride from Aldrich was recrystallized with a known procedure.[50] Triethylamine, methylene chloride, benzene, and acetonitrile were predried with CaH_2 and distilled from P_2O_5. 2-Ethyl-2-oxazoline was predried overnight with CaH_2 and distilled from fresh CaH_2. Pyridine was predried with KOH for 1 day and then distilled from KOH into KOH. Anhydrous ethyl ether, anhydrous ethyl alcohol, methanol, chloroform, and hexane were used as purchased. Methyl acrylate was washed two times with 5% NaOH, two times with 18Ω Millipore water, and was dried with $MgSO_4$ overnight to remove the inhibitor. Ethylenediamine was distilled before use. *n*-Butyl amine, *n*-hexyl amine, and *n*-octyl amine were predried with $MgSO_4$ and distilled from CaH_2 into KOH. *n*-Decyl amine was predried with $MgSO_4$ and vacuum-distilled from CaH_2, and *n*-dodecyl amine was only vacuum-distilled before use. Aqueous acid and base solutions were prepared in 18Ω Millipore water. Millipore Biomax 5000 NMWL poly(ether sulfone) and Millipore PLBC 3000 NMWL regenerated cellulose ultrafiltration membranes were flushed first with water and then with methanol before use to remove the glycerin and azide with which they were pretreated.

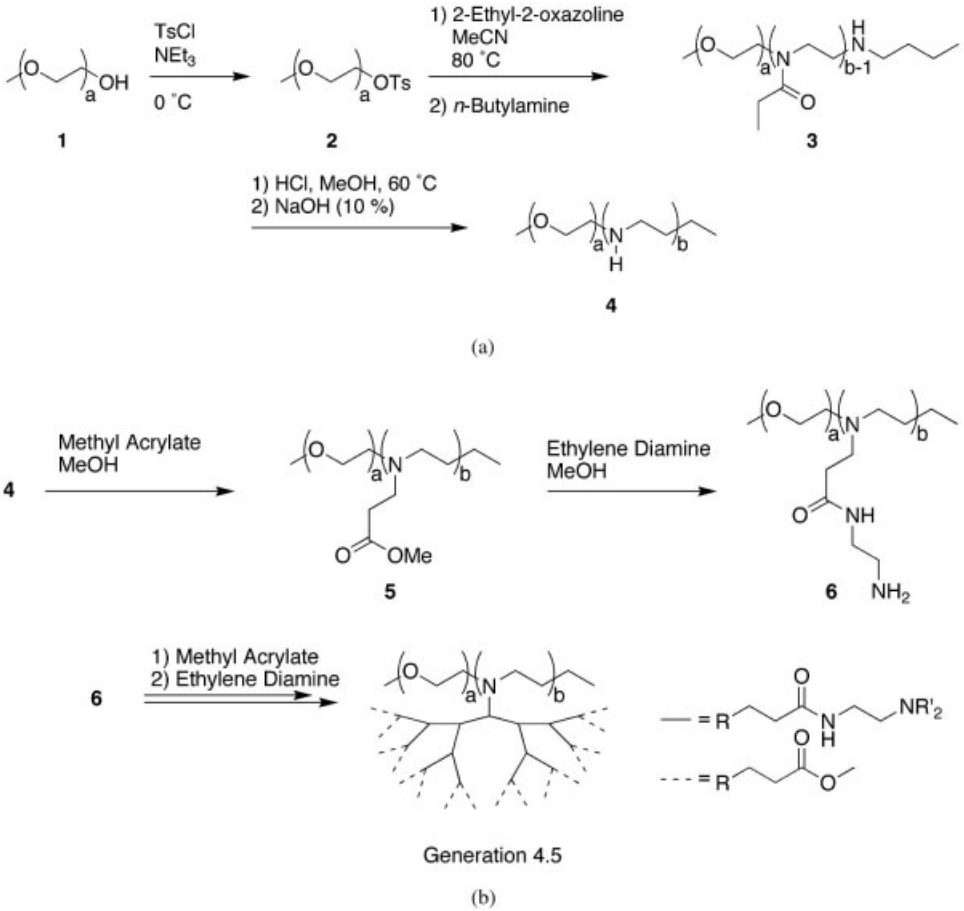

Figure 2. Synthetic schemes (a) used to prepare the PEO–PEI diblock copolymer backbone and (b) used to prepare the PEO–PEI–PAMAM linear–dendritic rod diblock copolymer.

Synthesis

The synthetic scheme used to prepare the desired linear–dendritic rod diblock copolymers is outlined in Figure 2(a,b). Figure 2(a) illustrates the synthesis of the PEO–LPEI backbone via the cationic polymerization of poly(2-ethyl 2-oxazoline) (PEOX) from the tosylate end group of a linear monodisperse PEO polymer chain, followed by hydrolysis of the PEOX block to form linear poly(ethylene imine) (LPEI). Figure 2(a) also shows the addition of the dendritic branches to the diblock copolymer backbone. These polymers were made amphiphilic through the addition of alkyl chains of various lengths to the half-generation methyl ester terminated branches of the dendritic block, as shown in Figure 3. The synthetic details for each of the polymers, as well as their chemical verification by ^{1}H NMR and Fourier transform infrared (FTIR), are given next; for all synthetic procedures, the reaction glassware was oven-dried before use, evacuated, and maintained in a nitrogen environment during synthesis.

Poly(ethylene oxide) Monomethyl Ether Tosylate (PEO-OTs)

PEO-OTs was prepared with a known procedure.[51] Methylene chloride (30 mL) was added to 14.23 g (0.0075 mol of polymer and hydroxyl groups) of predried methoxy-PEO-OH in a round-bottom flask, and the two were stirred for 5 min until the methoxy-PEO-OH dissolved. Triethylamine (3.1 mL, 0.022 mol) was added to the flask, which was subsequently immersed in an ice bath, and the solution was stirred for another 20 min. Tosyl chloride (4.07 g, 0.021 mol) was added to the cold, stirring solution through a solid funnel; the tosyl chloride slowly dissolved, leaving a clear,

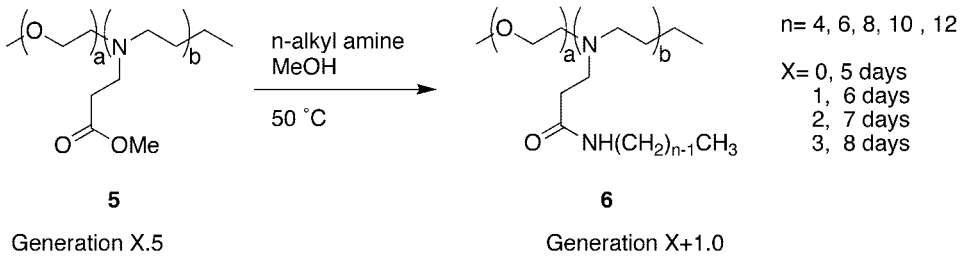

Figure 3. Synthetic scheme used to functionalize the methyl ester chain end of the linear–dendritic rod diblock copolymers with alkyl groups.

colorless solution. The solution was allowed to slowly warm to room temperature. During the reaction process, an insoluble white precipitate formed from the creation of triethylammonium chloride salts. After 12 h, the solution was filtered, and the filtrate was concentrated by vacuum distillation. The resulting white solid was redissolved with approximately 50 mL of benzene, and excess triethylammonium salts were removed by filtration. The resulting faint yellow filtrate solution was gently heated and stirred with Norit and silica gel to remove other impurities and then was filtered through a Celite bed packed in a size D glass filtration funnel. The liquor was then precipitated into 500 mL of stirring ether; the resulting white precipitate was collected by filtration. This product was reprecipitated twice in methylene chloride/ethyl ester, and the purified polymer was dried *in vacuo* for 2 days. The polymer was a powdery, white solid.

Yield: 9.20 g, 59%. ^{1}H NMR [dimethyl sulfoxide-d_6 (DMSO-d_6)]: 7.78 and 7.50 (C**H**s of aromatic ring), 4.11 (C**H$_2$**OTs), 3.51 (—O—C**H$_2$**—C**H$_2$**—), 3.24 (C**H$_3$**—O—), 2.43 (C**H$_3$** of tosylate). FTIR (ν, cm^{-1}): 2946, 2878, 2695, 1473, 1358, 1284, 1170, 1148, 1117, 1064, 949, 844, 810, 750.

Poly(ethylene oxide)–Poly(2-ethyl 2-oxazoline) (PEO–PEOX) Diblock Copolymer

2-Ethyl-2-oxazoline (15 mL, 0.15 mol) and 15 mL of acetonitrile were placed in a two-necked, 250-mL reaction flask. PEO-OTs (6.78 g; 0.0033 mol of polymer and tosyl groups) was dissolved in 15 mL of acetonitrile and transferred to an addition funnel with a syringe. The PEO-OTs/acetonitrile solution was added to the reaction flask, and the addition funnel was rinsed with an additional 15 mL of acetonitrile, for a total acetonitrile volume of 30 mL. The reaction flask was heated at approximately 80 °C for 48 h. The reaction solution was then cooled in an ice bath; afterward, 2 mL (0.020 mol) of *n*-butyl amine was added to terminate the reaction. After 12 h, the acetonitrile and excess *n*-butyl amine were removed by vacuum distillation. The resulting polymer was a colorless, transparent solid. The polymer was dissolved in a minimum of chloroform and precipitated into 1000 mL of ether. A white precipitate formed on the bottom of the flask, and the liquid was removed by decantation. The polymer was purified a second time by reprecipitation in chloroform/ether and was dried *in vacuo* for 2 days. The polymer was a white solid.

Yield: 21.21 g, 97%. ^{1}H NMR ($CDCl_3$): 3.66 (—O—C**H$_2$**—C**H$_2$**—), 3.47 (—N—C**H$_2$**—C**H$_2$**—), 2.42 and 2.33 (—CO—C**H$_2$**—CH_3), 1.14 (—CO—CH_2—C**H$_3$**). FTIR (ν, cm^{-1}): 2972, 2936, 2878, 1646, 1473, 1426, 1379, 1200, 1111, 823.

Poly(ethylene oxide)–Poly(ethylene imine) (PEO–PEI) Diblock Copolymer

The synthesis of the PEO–PEI diblock copolymer was accomplished by weak acid hydrolysis of the PEO–PEOX diblock copolymer with a modified procedure from Overberger and Peng.[52] PEO–PEOX (17.28 g; 0.0027 mol of polymer and 0.12 mol of amide groups) was placed in a single-necked, 2000-mL, round-bottom flask equipped with a condenser and a vacuum adapter in the neck and a stir bar in the bottom. A 6 N HCl solution (350 mL, 2.1 mol) and 350 mL of methanol were added to the reaction flask, and the solution was heated at 60 °C for 2 days. Afterward, the acidic solution was removed by vacuum distillation. The polymer was redissolved in 1000 mL of a 3 N HCl solution (3.0 mol), and the solution was again heated at 60 °C for another 3.5 days, at which time the polymer began to precipitate from solution. To ensure complete hydrolysis, the solution was heated for another 24 h at 60

°C. Afterward, the acidic solution was again removed by vacuum distillation. The resulting white PEO–PEI/H^+Cl^- salt was dissolved with approximately 350 mL of water, and insoluble solids were removed via filtration with a Büchner funnel. The acidic polymer solution was neutralized by the addition of approximately 150 mL of a 10% NaOH solution, which yielded a pH of 14; the polymer precipitated from solution as fine, white suspended particles. The polymer was collected on a Büchner funnel fitted with standard filter paper and washed thoroughly with chloroform to remove unreacted PEO and low-molecular-weight diblock copolymer. This chloroform wash was repeated a second time. The polymer was recrystallized twice in water and was collected by vacuum filtration through a size D glass filtration funnel. The light yellow, solid polymer was heated *in vacuo* at 110 °C for 6 h to remove residual water. After the polymer melt stopped bubbling, the heat was removed, and the polymer was dried at room temperature for another 2 days. The resulting polymer was a clear, light yellow solid.

Yield: 6.64 g, 40%. ^{1}H NMR (MeOH-*d*): 3.65 (—O—C**H$_2$**—C**H$_2$**—), 2.75 (—NH—C**H$_2$**—C**H$_2$**—). FTIR (ν, cm^{-1}): 3219, 2907, 2877, 2810, 2734, 1452, 1334, 1135, 1111, 803.

There was a large increase in the ^{1}H NMR (PEOX/PEI)/PEO block integration ratios during the conversion of PEO–PEOX into the PEO–PEI diblock copolymer from 1.37 to 2.32. This increase was the result of removing PEO that had not initiated the polymerization of the second block or that had only formed a short PEOX/PEI block such that the polymers were still soluble in water and chloroform and were removed during the purification of the PEO–PEI polymer. This increase was not caused by degradation of the PEO block in the acidic environment; when a PEO homopolymer blank was subjected to the same acidic reaction conditions, little or no change in the molecular weight and polydispersity of the polymer was observed with size exclusion chromatography (SEC) before and after exposure.

PEO–PEI Dendritic Diblock Generation 0.5

PEO–PEI (5.21 g; 8.5×10^{-4} mol of polymer and 0.083 mol of amine groups) was dissolved in 40 mL of methanol. Methyl acrylate (20 mL, 0.22 mol) was added to a three-necked, 250-mL, round-bottom flask equipped with an addition funnel and a condenser and was subsequently chilled in an ice bath for 15 min. All of the polymer/methanol solution was transferred to an addition funnel and was added dropwise over 35 min. The addition funnel was rinsed with an additional 27 mL of methanol for a total methanol volume of 67 mL. The reaction flask was covered with aluminum foil to prevent the polymer from yellowing, and the solution was allowed to warm to room temperature. After 48 h, the majority of the methanol and the excess methyl acrylate were removed by vacuum distillation, and the polymer was left to dry *in vacuo* for 2 days. The polymer was dissolved in a minimum of chloroform and was purified by reprecipitation in approximately 475 mL of hexanes. After stirring overnight, the polymer formed an opaque, yellow paste on the bottom of the flask. The chloroform and hexanes were removed by decantation, and the polymer was allowed to dry *in vacuo* for another 2 days. The polymer was a yellow, waxy solid.

Yield: 11.90 g, 97%. ^{1}H NMR (MeOH-*d*): 3.69 (—CH_2—CH_2—CO—OC**H$_3$**), 3.65 (—O—C**H$_2$**—C**H$_2$**—), 2.85 (—C**H$_2$**—CH_2—CO—OCH_3), 2.61 (—N—C**H$_2$**—C**H$_2$**—), 2.53 (—CH_2—C**H$_2$**—CO—OCH_3). FTIR (ν, cm^{-1}): 2948, 2820, 1733, 1436, 1257, 1196, 1114, 1038, 844.

PEO–PEI Dendritic Diblock Generation 1.0

Ethylenediamine (2550 mL) and 850 mL of methanol were placed in two three-necked, 5000-mL, round-bottom flasks equipped with addition funnels, for a total ethylenediamine volume of 5100 mL (76.3 mol) and a total methanol volume of 1700 mL. The flasks and the ethylenediamine/methanol solution were chilled in an ice bath overnight. Two portions of the PEO–PEI generation 0.5 polymer, one of 2.13 g (1.5×10^{-4} mol of polymer and 0.014 mol of ester groups) and the other of 2.12 g (1.4×10^{-4} mol of polymer and 0.014 mol of ester groups), were each dissolved in 20 mL of methanol and added dropwise over 45–50 min to each of the two reaction flasks with addition funnels; this was followed by a rinse of 10 mL of methanol. The total volume of the polymer/methanol solution used in the reaction was 40 mL (4.25 g of polymer, 2.9×10^{-4} mol of polymer, 0.028 mol of ester groups). The two reaction flasks were covered with glass wool to keep the polymer from yellowing, and the solutions were stirred in ice baths for 5 days at temperatures between 5 and 12 °C. Afterward, the majority of the methanol and excess ethylenediamine were removed by vacuum distillation, and the polymer was left to dry *in vacuo* for 2 days. The

polymer was redissolved in methanol and was purified by ultrafiltration in methanol through a Biomax 5000 NMWL poly(ether sulfone) membrane. Unfortunately, some of the polymer passed through the membrane, so the polymer/methanol solution that passed through the membrane was concentrated by vacuum distillation, redissolved in methanol, and purified a second time by ultrafiltration. The two pure polymer fractions from ultrafiltration were concentrated by vacuum distillation, and the polymer was again dried *in vacuo* for another 1.5 days. The polymer was a clear, light yellow, glassy solid. All the purified amine-terminated, whole-generation polymers were stored as methanol solutions after synthesis and before characterization to prevent the polymers from crosslinking upon standing. The polymer was a clear, light yellow, glassy solid.

Yield: 4.16 g, 82%. ^{1}H NMR (MeOH-*d*): 3.65 (—O—C**H$_2$**—C**H$_2$**—), 3.28 (—CO—NH—C**H$_2$**—CH_2—NH_2), 2.85 (—N—C**H$_2$**—CH_2—CO—NH—), 2.75 (—CO—NH—CH_2—C**H$_2$**—NH_2), 2.62 (—N—C**H$_2$**—C**H$_2$**—), 2.41 (—N—CH_2—C**H$_2$**—CO—NH—). FTIR (ν, cm^{-1}): 3255, 3058, 2935, 2830, 1654, 1555, 1475, 1346, 1112, 822.

PEO–PEI Dendritic Diblock Generation 1.5

The PEO–PEI generation 1.0 polymer (4.16 g; 2.4 $\times$ 10^{-4} mol of polymer and 0.023 mol of amine groups) was dissolved in 43 mL of methanol. The polymer dissolved slowly over several hours. Methyl acrylate (10 mL, 0.11 mol) and 20 mL of methanol were added to a two-necked, 250-mL, round-bottom flask equipped with an addition funnel and a condenser and were subsequently chilled in an ice bath for 15 min. The polymer/methanol solution (37.5 mL; 3.63 g of polymer, 2.1 $\times$ 10^{-4} mol of polymer, and 0.021 mol of amine groups) and 20 mL of methanol were transferred to an addition funnel and were added dropwise over 40 min. The addition funnel was rinsed with an additional 13 mL of methanol for a total methanol volume of 90 mL. After the reaction solution warmed to room temperature and was stirred for 48 h, the polymer was recovered and purified as described for PEO–PEI dendritic diblock generation 0.5. The polymer was a yellow, viscous liquid.

Yield: 5.91 g, 83%. ^{1}H NMR (MeOH-*d*): 3.69 (—CH_2—CH_2—CO—OC**H$_3$**), 3.65 (—O—C**H$_2$**—C**H$_2$**—), 3.27 (—CO—NH—C**H$_2$**—CH_2—N<), 2.87 (—C**H$_2$**—CH_2—CO—NH—), 2.80 (—C**H$_2$**—CH_2—CO—OCH_3), 2.66 (—N—C**H$_2$**—C**H$_2$**—), 2.59 (—CO—NH—CH_2—C**H$_2$**—N<), 2.49 (—CH_2—C**H$_2$**—CO—OCH_3), 2.42 (—CH_2—C**H$_2$**—CO—NH—). FTIR (ν, cm^{-1}): 3303, 3071, 2952, 2820, 1740, 1652, 1542, 1438, 1362, 1258, 1202, 1043, 847.

PEO–PEI Dendritic Diblock Generation 2.0

Ethylenediamine (2780 mL) and 840 mL of methanol were placed in three three-necked, 5000-mL, round-bottom flasks equipped with addition funnels, for a total ethylenediamine volume of 8340 mL (124.8 mol) and a total methanol volume of 2520 mL. The flasks and the ethylenediamine/methanol solutions were chilled in ice baths overnight. The PEO–PEI generation 1.5 polymer (3.78 g; 1.1 $\times$ 10^{-4} mol of polymer and 0.022 mol of ester groups) was dissolved in 60 mL of methanol. A 20-mL portion of the polymer/methanol solution was transferred to each of the three addition funnels, and the polymer/methanol solutions were added dropwise to the ethylenediamine/methanol solutions over 15–20 min. The three reaction flasks were covered with glass wool to prevent the polymer from yellowing, and the solutions were stirred in ice baths for 6 days at temperatures between 5 and 12 °C. Afterward, the polymer was recovered as described for PEO–PEI dendritic diblock generation 1.0, except that the second time the polymer/methanol solution was ultrafiltered, a PLBC 3000 NMWL regenerated cellulose ultrafiltration membrane was used. The polymer was a clear, yellow, glassy solid.

Yield: 3.92 g, 89%. ^{1}H NMR (MeOH-*d*): 3.65 (—O—C**H$_2$**—C**H$_2$**—), 3.28 (—CO—NH—C**H$_2$**—CH_2—N< and —CO—NH—C**H$_2$**—CH_2—NH_2), 2.82 (—C**H$_2$**—CH_2—CO—NH—), 2.77 (—CO—NH—CH_2—C**H$_2$**—NH_2), 2.62 (—N—C**H$_2$**—C**H$_2$**— and —CO—NH—CH_2—C**H$_2$**—N<), 2.40 (—CH_2—C**H$_2$**—CO—NH—). FTIR (ν, cm^{-1}): 3261, 3058, 2938, 2823, 1652, 1548, 1466, 1334, 1252, 1110, 1039, 820.

PEO–PEI Dendritic Diblock Generation 2.5

The PEO–PEI generation 2.0 polymer (3.91 g; 1.0 $\times$ 10^{-4} mol of polymer and 0.01931 mol of amine groups) was dissolved in 80 mL of methanol. The polymer dissolved over several hours. Methyl acrylate (10 mL, 0.11 mol) and 20 mL of methanol were added to a two-necked, 250-mL, round-bottom flask equipped with an addition funnel and a condenser and were subsequently chilled in an ice bath for 25 min. The polymer/methanol solution (71 mL; 3.47 g of polymer, 8.8 $\times$ 10^{-5} mol of polymer, 0.017 mol of amine groups) was trans-

ferred to an addition funnel and was added dropwise over 40 min. The addition funnel was rinsed with an additional 5 mL of methanol for a total methanol volume of 96 mL. After the reaction solution warmed to room temperature and was stirred for 48 h, the polymer was recovered and purified as described for PEO–PEI dendritic diblock generation 0.5. The polymer was a golden yellow, very viscous liquid.

Yield: 5.29 g, 82%. ^{1}H NMR (MeOH-*d*): 3.69 (—CH_2—CH_2—CO—O$C\mathbf{H_3}$), 3.65 (—O—$C\mathbf{H_2}$—$C\mathbf{H_2}$—), 3.28 (—CO—NH—$C\mathbf{H_2}$—CH_2—N<), 2.85 (—$C\mathbf{H_2}$—CH_2—CO—NH), 2.79 (—$C\mathbf{H_2}$—CH_2—CO—OCH_3), 2.64 (—N—$C\mathbf{H_2}$—$C\mathbf{H_2}$— and —CO—NH—CH_2—$C\mathbf{H_2}$—N<) next to a whole branch, 2.58 (—CO—NH—CH_2—$C\mathbf{H_2}$—N<) next to a half-branch, 2.49 (—CH_2—$C\mathbf{H_2}$—CO—OCH_3), 2.41 (—CH_2—$C\mathbf{H_2}$—CO—NH—). FTIR (ν, cm^{-1}): 3272, 3064, 2944, 2823, 1739, 1646, 1542, 1433, 1362, 1258, 1203, 1050, 842.

PEO–PEI Dendritic Diblock Generation 3.0

Ethylenediamine (3000 mL) and 775 mL of methanol were placed in three three-necked, 5000-mL, round-bottom flasks equipped with addition funnels, for a total ethylenediamine volume of 9000 mL (134.6 mol) and a total methanol volume of 2325 mL. The flasks and the ethylenediamine/methanol solutions were chilled in ice baths overnight. The PEO–PEI generation 2.5 polymer (3.43 g; 4.7×10^{-5} mol of polymer and 0.018 mol of ester groups) was dissolved in 64 mL of methanol. A 20-mL portion of the polymer/methanol solution was transferred to each of the three addition funnels, and the polymer/methanol solutions were added dropwise to the ethylenediamine/methanol solutions over 40–45 min. The total volume of the polymer/methanol solution used in the reaction was 60 mL (3.22 g of polymer, 4.4×10^{-5} mol of polymer, and 0.017 mol of ester groups.) The three reaction flasks were covered with glass wool to prevent the polymer from yellowing, and the solutions were stirred in ice baths for 7 days at temperatures between 5 and 12 °C. Afterward, the polymer was recovered as described for PEO–PEI dendritic diblock generation 2.0. The polymer was a clear, orange, glassy solid.

Yield: 3.80 g, 100%. ^{1}H NMR (MeOH-*d*): 3.65 (—O—$C\mathbf{H_2}$—$C\mathbf{H_2}$—), 3.28 (—CO—NH—$C\mathbf{H_2}$—CH_2—N< and —CO—NH—$C\mathbf{H_2}$—CH_2—NH_2), 2.81 (—$C\mathbf{H_2}$—CH_2—CO—NH—), 2.75 (—CO—NH—CH_2—$C\mathbf{H_2}$—NH_2), 2.60 (—N—$C\mathbf{H_2}$—$C\mathbf{H_2}$— and —CO—NH—CH_2—$C\mathbf{H_2}$—N<), 2.39 (—CH_2—$C\mathbf{H_2}$—CO—NH—). FTIR (ν, cm^{-1}): 3268, 3063, 2930, 2835, 1648, 1554, 1465, 1438, 1349, 1282, 1243, 1149, 1038, 689.

PEO–PEI Dendritic Diblock Generation 3.5

The PEO–PEI generation 3.0 polymer (3.80 g; 4.5×10^{-5} mol of polymer and 0.018 mol of amine groups) was dissolved in 70 mL of methanol. The polymer dissolved slowly over several hours. Methyl acrylate (10 mL, 0.111 mol) and 20 mL of methanol were added to a two-necked, 250-mL, round-bottom flask equipped with an addition funnel and condenser and were subsequently chilled in an ice bath for 25 min. The polymer/methanol solution (60 mL; 3.25 g of polymer, 3.9×10^{-5} mol of polymer, and 0.015 mol of amine groups) was transferred to an addition funnel and was added dropwise to the methyl acrylate/methanol solution over 35 min. The addition funnel was rinsed with an additional 17 mL of methanol for a total methanol volume of 97 mL. After the reaction solution warmed to room temperature and was stirred for 60 h, the polymer was recovered and purified as described for PEO–PEI dendritic diblock generation 0.5. The polymer was an orange, very viscous liquid.

Yield: 4.89 g, 84%. ^{1}H NMR (MeOH-*d*): 3.69 (—CH_2—CH_2—CO—O$C\mathbf{H_3}$), 3.65 (—O—$C\mathbf{H_2}$—$C\mathbf{H_2}$—), 3.28 (—CO—NH—$C\mathbf{H_2}$—CH_2—N<), 2.85 (—$C\mathbf{H_2}$—CH_2—CO—NH—), 2.79 (—$C\mathbf{H_2}$—CH_2—CO—OCH_3), 2.64 (—N—$C\mathbf{H_2}$—$C\mathbf{H_2}$— and —CO—NH—CH_2—$C\mathbf{H_2}$—N<) next to a whole branch, 2.58 (—CO—NH—CH_2—$C\mathbf{H_2}$—N<) next to a half-branch, 2.49 (—CH_2—$C\mathbf{H_2}$—CO—OCH_3), 2.41 (—CH_2—$C\mathbf{H_2}$—CO—NH—). FTIR (ν, cm^{-1}): 3288, 3069, 2951, 2823, 1736, 1651, 1544, 1437, 1367, 1255, 1196, 1046, 843.

PEO–PEI Dendritic Diblock Generation 4.0

Ethylenediamine (3530 mL) and 1000 mL of methanol were placed in two three-necked, 5000-mL, round-bottom flasks equipped with an addition funnel, for a total ethylenediamine volume of 7060 mL (105.6 mol) and a total methanol volume of 2000 mL. The flasks and the ethylenediamine/methanol solutions were chilled in ice baths overnight. The PEO–PEI generation 3.5 polymer (3.02 g; 2.0×10^{-5} mol of polymer and 0.016 mol of ester groups) was dissolved in 60 mL of methanol. A 20-mL portion of the polymer/methanol solution was transferred to each of the two addition funnels, and the polymer/methanol solutions were added dropwise to the ethylenediamine/

methanol solutions over 70 min. The total volume of the polymer/methanol solution used in the reaction was 40 mL (2.02 g of polymer, 1.3×10^{-5} mol of polymer, and 0.010 mol of ester groups.) Each of the addition funnels was rinsed with an additional 35 mL of methanol for a total methanol volume of 2110 mL. The two reaction flasks were covered with glass wool to prevent the polymer from yellowing, and the solutions were stirred in ice baths for 8 days at temperatures between 5 and 12 °C. Afterward, the polymer was recovered as described for PEO–PEI dendritic diblock generation 2.0. The polymer was a clear, brown, glassy solid.

Yield: 2.58 g, 100%. ^{1}H NMR (MeOH-*d*): 3.65 (—O—C**H$_2$**—C**H$_2$**—), 3.28 (—CO—NH—C**H$_2$**—CH_2—N< and —CO—NH—C**H$_2$**—CH_2—NH_2), 2.81 (—C**H$_2$**—CH_2—CO—NH), 2.75 (—CO—NH—CH_2—C**H$_2$**—NH_2), 2.60 (—N—C**H$_2$**—C**H$_2$**— and —CO—NH—CH_2—C**H$_2$**—N<), 2.39 (—CH_2—C**H$_2$**—CO—NH—). FTIR (ν, cm^{-1}): 3257, 3057, 2930, 2819, 1648, 1543, 1460, 1432, 1349, 1243, 1149, 1033.

PEO–PEI Dendritic Diblock Generation 4.5

The PEO–PEI generation 4.0 polymer (2.58 g; 1.5×10^{-5} mol of polymer and 0.012 mol of amine groups) was dissolved in 80 mL of methanol. The polymer dissolved very slowly over 60 h. During this time, the polymer/methanol solution was sonicated a total of 4 h to increase the dissolution rate. Methyl acrylate (5 mL, 0.056 mol) and 10 mL of methanol were added to a two-necked, 250-mL, round-bottom flask equipped with an addition funnel and a condenser and were subsequently chilled in an ice bath for 25 min. The polymer/methanol solution (60 mL; 1.94 g of polymer, 1.134×10^{-5} mol of polymer, and 0.0087 mol of amine groups) was transferred to an addition funnel and was added dropwise to the methyl acrylate/methanol solution over 1.5 h. The addition funnel was rinsed with an additional 5 mL of methanol for a total methanol volume of 75 mL. After the reaction solution warmed to room temperature and was stirred for 60 h, the polymer was recovered and purified as described for generation 0.5. The polymer was a brown, soft, sticky solid.

Yield: 3.30 g, 96%. ^{1}H NMR (MeOH-*d*): 3.69 (—CH_2—CH_2—CO—O**CH$_3$**), 3.65 (—O—C**H$_2$**—C**H$_2$**—), 3.28 (—CO—NH—C**H$_2$**—CH_2—N<), 2.84 (—C**H$_2$**—CH_2—CO—NH—), 2.79 (—C**H$_2$**—CH_2—CO—OCH_3), 2.64 (—N—C**H$_2$**—C**H$_2$**— and —CO—NH—CH_2—C**H$_2$**—N<) next to a whole branch, 2.58 (—CO—NH—CH_2—C**H$_2$**—N<) next to a half-branch, 2.49 (—CH_2—C**H$_2$**—CO—OCH_3), 2.40 (—CH_2—C**H$_2$**—CO—NH—). FTIR (ν, cm^{-1}): 3285, 3066, 2954, 2832, 1738, 1648, 1546, 1439, 1359, 1263, 1199, 1050, 847, 751.

End-Group Modification

PEO–PEI Dendritic Diblock Generation 1.0: Butyl-Terminated

n-Butyl amine (20 mL, 0.20 mol) and 20 mL of methanol were added to a two-necked, 250-mL, round-bottom flask equipped with an addition funnel and a condenser and were subsequently chilled in an ice bath for 5 min. The PEO–PEI generation 0.5 polymer (0.50 g; 3.5×10^{-5} mol of polymer and 0.0034 mol of ester groups) was dissolved with 20 mL of methanol, transferred to an addition funnel, and added dropwise over 10 min. The addition funnel was rinsed with an additional 5 mL of methanol for a total methanol volume of 45 mL. The reaction flask was covered with aluminum foil to prevent the polymer from yellowing, and the solution was allowed to warm to room temperature. After 24 h, an oil bath was placed beneath the reaction flask, and the solution was heated at 40 °C. After 4 days of heating, the majority of the methanol and excess *n*-butyl amine were removed by vacuum distillation, and the polymer was left to dry *in vacuo* for 2 days. The polymer was purified twice by reprecipitation in chloroform/ethyl ether to remove traces of *n*-butyl amine. The polymer was again dried *in vacuo* for another 2 days. The polymer was a light yellow, very viscous liquid.

Yield: 0.47 g, 73%. Substitution: 98%. ^{1}H NMR (MeOH-*d*): 3.69 (unreacted —CH_2—CH_2—CO—O**CH$_3$**), 3.65 (—O—C**H$_2$**—C**H$_2$**—), 3.20 (—CO—NH—C**H$_2$**—CH_2—CH_2—CH_3), 2.84 (—C**H$_2$**—CH_2—CO—NH—), 2.62 (—N—C**H$_2$**—C**H$_2$**—), 2.38 (—CH_2—C**H$_2$**—CO—NH—), 1.51 (—CO—NH—CH_2—C**H$_2$**—CH_2—CH_3), 1.38 (—CO—NH—CH_2—CH_2—C**H$_2$**—CH_3), 0.94 (—CO—NH—CH_2—CH_2—CH_2—C**H$_3$**). FTIR (ν, cm^{-1}): 3280, 3065, 2958, 2928, 2866, 2810, 1738, 1646, 1554, 1467, 1115.

PEO–PEI Dendritic Diblock Generation 1.0: Hexyl-Terminated

The procedure was identical to that for the aforementioned butyl-terminated species. *n*-Hexyl

amine (25 mL, 0.19 mol) and 20 mL of methanol were added to a round-bottom flask and were subsequently chilled in an ice bath for 10 min. The PEO–PEI generation 0.5 polymer (0.50 g; 3.5×10^{-5} mol of polymer and 0.0034 mol of ester groups) was dissolved with 20 mL of methanol, transferred to an addition funnel, and added dropwise over 10 min. The addition funnel was rinsed with an additional 11 mL of methanol for a total methanol volume of 51 mL. The polymer was a light yellow, very viscous liquid.

Yield: 0.45 g, 62%. Substitution: 95%. ^{1}H NMR (MeOH-*d*): 3.69 (unreacted —CH_2—CH_2—CO—O$C\mathbf{H_3}$), 3.65 (—O—$C\mathbf{H_2}$—$C\mathbf{H_2}$—), 3.19 [—CO—NH—$C\mathbf{H_2}$—CH_2—$(CH_2)_3$—CH_3], 2.81 (—$C\mathbf{H_2}$—CH_2—CO—NH—), 2.61 (—N—$C\mathbf{H_2}$—$C\mathbf{H_2}$—), 2.37 (—CH_2—$C\mathbf{H_2}$—CO—NH—), 1.51 [—CO—NH—CH_2—$C\mathbf{H_2}$—$(CH_2)_3$—CH_3], 1.34 [—CO—NH—CH_2—CH_2—$(C\mathbf{H_2})_3$—CH_3], 0.94 [—CO—NH—CH_2—CH_2—$(CH_2)_3$—$C\mathbf{H_3}$]. FTIR (ν, cm^{-1}): 3285, 3071, 2953, 2922, 2856, 2815, 1743, 1651, 1549, 1462, 1115.

PEO–PEI Dendritic Diblock Generation 1.0: Octyl-Terminated

The procedure was identical to that for the aforementioned butyl-terminated species. *n*-Octyl amine (32 mL, 0.19 mol) and 20 mL of methanol were added to a round-bottom flask and were subsequently chilled in an ice bath for 10 min. The PEO–PEI generation 0.5 polymer (0.51 g; 3.5×10^{-5} mol of polymer and 0.0034 mol of ester groups) was dissolved with 20 mL of methanol, transferred to an addition funnel, and added dropwise over 10 min. The addition funnel was rinsed with an additional 25 mL of methanol for a total methanol volume of 65 mL. The polymer was a light yellow, very viscous liquid.

Yield: 0.18 g, 23%. Substitution: 87%. ^{1}H NMR (MeOH-*d*): 3.70 (unreacted —CH_2—CH_2—CO—O$C\mathbf{H_3}$), 3.65 (—O—$C\mathbf{H_2}$—$C\mathbf{H_2}$—), 3.19 [—CO—NH—$C\mathbf{H_2}$—CH_2—$(CH_2)_5$—CH_3], 2.82 (—$C\mathbf{H_2}$—CH_2—CO—NH—), 2.62 (—N—$C\mathbf{H_2}$—$C\mathbf{H_2}$—), 2.50 (unreacted —CH_2—$C\mathbf{H_2}$—CO—OCH_3), 2.38 (—CH_2—$C\mathbf{H_2}$—CO—NH—), 1.51 [—CO—NH—CH_2—$C\mathbf{H_2}$—$(CH_2)_5$—CH_3], 1.34 [—CO—NH—CH_2—CH_2—$(C\mathbf{H_2})_5$—CH_3], 0.93 [—CO—NH—CH_2—CH_2—$(CH_2)_5$—$C\mathbf{H_3}$]. FTIR (ν, cm^{-1}): 3280, 3071, 2950, 2922, 2856, 2815, 1743, 1646, 1554, 1462, 1115.

PEO–PEI Dendritic Diblock Generation 1.0: Decyl-Terminated

The procedure was identical to that for the aforementioned butyl-terminated species, except that a different purification procedure was used. *n*-Decyl amine (23 mL, 0.12 mol) and 20 mL of methanol were added to a round-bottom flask and were subsequently chilled in an ice bath for 20 min. The PEO–PEI generation 0.5 polymer (0.50 g; 3.5×10^{-5} mol of polymer and 0.0034 mol of ester groups) was dissolved with 10 mL of methanol, transferred to an addition funnel, and added dropwise over 5 min. The addition funnel was rinsed with an additional 16 mL of methanol for a total methanol volume of 46 mL. After heating and vacuum distillation, the polymer was redissolved in methanol and was purified by ultrafiltration through a PLBC 3000 NMWL regenerated cellulose membrane to remove traces of *n*-decyl amine. The pure polymer/methanol ultrafiltration solution was concentrated by vacuum distillation, and the polymer was dried for another 1.5 days. The polymer was a light yellow, very viscous liquid.

Yield: 0.52 g, 58%. Substitution: 93%. ^{1}H NMR (MeOH-*d*): 3.70 (unreacted —CH_2—CH_2—CO—O$C\mathbf{H_3}$), 3.65 (—O—$C\mathbf{H_2}$—$C\mathbf{H_2}$—), 3.19 [—CO—NH—$C\mathbf{H_2}$—CH_2—$(CH_2)_7$—CH_3], 2.81 (—$C\mathbf{H_2}$—CH_2—CO—NH—), 2.61 (—N—$C\mathbf{H_2}$—$C\mathbf{H_2}$—), 2.38 (—CH_2—$C\mathbf{H_2}$—CO—NH—), 1.53 [—CO—NH—CH_2—$C\mathbf{H_2}$—$(CH_2)_7$—CH_3], 1.32 [—CO—NH—CH_2—CH_2—$(C\mathbf{H_2})_7$—CH_3], 0.93 [—CO—NH—CH_2—CH_2—$(CH_2)_7$—$C\mathbf{H_3}$]. FTIR (ν, cm^{-1}): 3285, 3071, 2952, 2922, 2856, 2815, 1743, 1646, 1549, 1462, 1355, 1115, 724.

PEO–PEI Dendritic Diblock Generation 1.0: Dodecyl-Terminated

The procedure was identical to that for the aforementioned decyl-terminated species. *n*-Dodecyl amine (13.74 g, 0.074 mol) was dissolved with 15 mL of methanol in a 125-mL Erlenmeyer flask and was subsequently added to a round-bottom flask. The solution was cooled in an ice bath for 15 min. The PEO–PEI generation 0.5 polymer (0.51 g; 3.5×10^{-5} mol of polymer and 0.0034 mol of ester groups) was dissolved with 10 mL of methanol, transferred to an addition funnel, and added dropwise over 5 min. The addition funnel was rinsed with an additional 5 mL of methanol for a total methanol volume of 30 mL. The polymer was a light yellow, soft solid.

Yield: 0.53 g, 55%. Substitution: 90%. ^{1}H NMR (MeOH-*d*): 3.70 (unreacted —CH_2—CH_2—CO—O**CH_3**), 3.65 (—O—**CH_2**—**CH_2**—), 3.19 [—CO—NH—**CH_2**—CH_2—$(CH_2)_9$—CH_3], 2.79 (—**CH_2**—CH_2—CO—NH—), 2.61 (—N—**CH_2**—**CH_2**—), 2.37 (—CH_2—**CH_2**—CO—NH—), 1.53 [—CO—NH—CH_2—**CH_2**—$(CH_2)_9$—CH_3], 1.32 [—CO—NH—CH_2—CH_2—$(CH_2)_9$—CH_3], 0.93 [—CO—NH—CH_2—CH_2—$(CH_2)_9$—**CH_3**]. FTIR (ν, cm^{-1}): 3288, 3071, 2950, 2920, 2855, 2817, 1738, 1646, 1553, 1461, 1353, 1114, 724.

PEO–PEI Dendritic Diblock Generation 1.0: Octadecyl-Terminated

n-Octadecyl amine (5.88 g, 0.022 mol) and 20 mL of methanol were placed in a two-necked, 100-mL, round-bottom flask equipped with an addition funnel and a condenser. The *n*-octadecyl amine did not dissolve with stirring, so the flask was heated; this induced dissolution. The flask was allowed to cool to room temperature. A small amount of octadecyl amine fell back out of solution, as indicated by the formation of a white precipitate on the bottom of the flask; however, the majority of the *n*-octadecyl amine remained in solution. The PEO–PEI generation 0.5 polymer (0.50 g; 3.4×10^{-5} mol of polymer and 0.0033 mol of ester groups) was dissolved with 5 mL of methanol, transferred to an addition funnel, and added dropwise over 5 min at room temperature. The addition funnel was rinsed with an additional 5 mL of methanol for a total methanol volume of 30 mL. The reaction flask was covered with aluminum foil to prevent the polymer from yellowing, and the solution was allowed to react at room temperature. After 24 h, an oil bath was placed beneath the reaction flask, and the solution was heated at 40 °C. After 3 days of heating at 40 °C, the solution became cloudy. The reaction temperature was increased to 60 °C, and this induced dissolution; the solution was left to stir at 60 °C for another 2.5 days. The methanol was removed by vacuum distillation, and the polymer was left to dry *in vacuo* for 1 day. The polymer was redissolved in methanol, and with time and exposure to air, the octadecyl amine fell out of solution as a white precipitate. The precipitate was removed by repeated vacuum filtration until no more precipitate appeared. The polymer/methanol solution was then purified by ultrafiltration in methanol through a PLBC 3000 NMWL regenerated cellulose membrane to remove traces of *n*-octadecyl amine. The pure polymer/methanol ultrafiltration solution was concentrated by vacuum distillation, and the polymer was again dried *in vacuo* for another day. The polymer was an off-white solid.

Yield: 0.19 g, 15%. Substitution: 95%. ^{1}H NMR ($CDCl_3$): 3.68 (unreacted —CH_2—CH_2—CO—O**CH_3**), 3.66 (—O—**CH_2**—**CH_2**—), 3.21 [—CO—NH—**CH_2**—CH_2—$(CH_2)_{15}$—CH_3], 2.76 (—**CH_2**—CH_2—CO—NH—), 2.64 (—N—**CH_2**—**CH_2**—), 2.33 (—CH_2—**CH_2**—CO—NH—), 1.50 [—CO—NH—CH_2—**CH_2**—$(CH_2)_{15}$—CH_3], 1.27 [—CO—NH—CH_2—CH_2—$(CH_2)_{15}$—CH_3], 0.90 [—CO—NH—CH_2—CH_2—$(CH_2)_{15}$—**CH_3**]. FTIR (ν, cm^{-1}): 3270, 3062, 2957, 2913, 2842, 2809, 1640, 1547, 1470, 1349, 1113, 751.

All the remaining *n*-alkyl-terminated PEO–PEI diblocks of generations 2–4 were synthesized in a manner similar to the methods described previously for generation 1 diblocks, with variations in the reaction time, temperature, and molar excess used. In particular, whereas the generation 2.0 butyl polymer was heated at 40 °C for 4 days, the other generation 2.0 alkyl-terminated polymers were heated at 45 °C for 5 days; the generation 3.0 and 4.0 butyl-to-dodecyl-terminated polymers were heated at 47–50 °C for 6 and 7 days, respectively. The generation 2.0, 3.0, and 4.0 octadecyl-terminated polymers were heated at 60 °C for 5, 6, and 7 days, respectively. All the polymers were purified by ultrafiltration in methanol through a PLBC 3000 NMWL regenerated cellulose membrane because that method resulted in the highest yields of purified polymers. The yields and NMR data for each species are reported next.

PEO–PEI Dendritic Diblock Generation 2.0: Butyl-Terminated

Yellow, very viscous liquid. Yield: 0.32 g, 92%. Substitution: 82%. ^{1}H NMR (MeOH-*d*): 3.69 (unreacted —CH_2—CH_2—CO—O**CH_3**), 3.65 (—O—**CH_2**—**CH_2**—), 3.28 (—CO—NH—**CH_2**—CH_2—N<), 3.19 (—CO—NH—**CH_2**—CH_2—CH_2—CH_3), 2.84 (—**CH_2**—CH_2—CO—NH—CH_2—CH_2—N<), 2.81 (—**CH_2**—CH_2—CO—NH—CH_2—CH_2—CH_2—CH_3), 2.76 (unreacted —**CH_2**—CH_2—CO—OCH_3), 2.62 (—N—**CH_2**—**CH_2**— and —CO—NH—CH_2—**CH_2**—N<), 2.50 (unreacted —CH_2—**CH_2**—CO—OCH_3), 2.40 (—CH_2—**CH_2**—CO—NH—CH_2—CH_2—N<), 2.37 (—CH_2—**CH_2**—CO—NH—CH_2—CH_2—CH_2—CH_3), 1.51 (—CO—NH—CH_2—**CH_2**—CH_2—CH_3), 1.39 (—CO—NH—CH_2—CH_2—**CH_2**—CH_3), 0.96 (—CO—

NH—CH_2—CH_2—CH_2—C**H**$_3$). FTIR (ν, cm^{-1}): 3285, 3071, 2953, 2928, 2866, 2815, 1646, 1544, 1462, 1365, 1248, 1110, 752.

PEO–PEI Dendritic Diblock Generation 2.0: Hexyl-Terminated

Yellow, very viscous liquid. Yield: 0.34 g, 85%. Substitution: 98%. ^{1}H NMR (MeOH-*d*): 3.69 (unreacted —CH_2—CH_2—CO—OC**H**$_3$), 3.65 (—O—C**H**$_2$—C**H**$_2$—), 3.28 (—CO—NH—C**H**$_2$—CH_2—N<), 3.18 [—CO—NH—C**H**$_2$—CH_2—$(CH_2)_3$—CH_3], 2.84 (—C**H**$_2$—CH_2—CO—NH—CH_2—CH_2—N<), 2.81 [—C**H**$_2$—CH_2—CO—NH—CH_2—CH_2—$(CH_2)_3$—CH_3], 2.76 (unreacted —C**H**$_2$—CH_2—CO—OCH_3), 2.62 (—N—C**H**$_2$—C**H**$_2$— and —CO—NH—CH_2—C**H**$_2$—N<), 2.50 (unreacted —CH_2—C**H**$_2$—CO—OCH_3), 2.40 (—CH_2—C**H**$_2$—CO—NH—CH_2—CH_2—N<), 2.36 [—CH_2—C**H**$_2$—CO—NH—CH_2—CH_2—$(CH_2)_3$—CH_3], 1.52 [—CO—NH—CH_2—C**H**$_2$—$(CH_2)_3$—CH_3], 1.34 [—CO—NH—CH_2—CH_2—(C**H**$_2$)$_3$—CH_3], 0.93 [—CO—NH—CH_2—CH_2—$(CH_2)_3$—C**H**$_3$]. FTIR (ν, cm^{-1}): 3281, 3073, 2957, 2920, 2853, 2820, 1739, 1646, 1547, 1459, 1364, 1248, 1119, 724, 685.

PEO–PEI Dendritic Diblock Generation 2.0: Octyl-Terminated

Yellow, very viscous liquid. Yield: 0.43 g, 93%. Substitution: 96%. ^{1}H NMR (MeOH-*d*): 3.69 (unreacted —CH_2—CH_2—CO—OC**H**$_3$), 3.65 (—O—C**H**$_2$—C**H**$_2$—), 3.28 (—CO—NH—C**H**$_2$—CH_2—N<), 3.18 [—CO—NH—C**H**$_2$—CH_2—$(CH_2)_5$—CH_3], 2.84 (—C**H**$_2$—CH_2—CO—NH—CH_2—CH_2—N<), 2.81 [—C**H**$_2$—CH_2—CO—NH—CH_2—CH_2—$(CH_2)_5$—CH_3], 2.76 (unreacted —C**H**$_2$—CH_2—CO—OCH_3), 2.62 (—N—C**H**$_2$—C**H**$_2$— and —CO—NH—CH_2—C**H**$_2$—N<), 2.50 (unreacted —CH_2—C**H**$_2$—CO—OCH_3), 2.40 (—CH_2—C**H**$_2$—CO—NH—CH_2—CH_2—N<), 2.36 [—CH_2—C**H**$_2$—CO—NH—CH_2—CH_2—$(CH_2)_5$—CH_3], 1.52 [—CO—NH—CH_2—C**H**$_2$—$(CH_2)_5$—CH_3], 1.34 [—CO—NH—CH_2—CH_2—(C**H**$_2$)$_5$—CH_3], 0.92 [—CO—NH—CH_2—CH_2—$(CH_2)_5$—C**H**$_3$]. FTIR (ν, cm^{-1}): 3280, 3071, 2954, 2922, 2856, 2817, 1738, 1641, 1548, 1460, 1356, 1279, 1245, 1120, 725.

PEO–PEI Dendritic Diblock Generation 2.0: Decyl-Terminated

Clear, yellow solid. Yield: 0.29 g, 86%. Substitution: 76%. ^{1}H NMR (MeOH-*d*): 3.69 (unreacted —CH_2—CH_2—CO—OC**H**$_3$), 3.65 (—O—C**H**$_2$—C**H**$_2$—), 3.28 (—CO—NH—C**H**$_2$—CH_2—N<), 3.18 [—CO—NH—C**H**$_2$—CH_2—$(CH_2)_7$—CH_3], 2.85 (—C**H**$_2$—CH_2—CO—NH—CH_2—CH_2—N<), 2.80 [—C**H**$_2$—CH_2—CO—NH—CH_2—CH_2—$(CH_2)_7$—CH_3], 2.76 (unreacted —C**H**$_2$—CH_2—CO—OCH_3), 2.63 (—N—C**H**$_2$—C**H**$_2$— and —CO—NH—CH_2—C**H**$_2$—N<), 2.50 (unreacted —CH_2—C**H**$_2$—CO—OCH_3), 2.40 (—CH_2—C**H**$_2$—CO—NH—CH_2—CH_2—N<), 2.36 [—CH_2—C**H**$_2$—CO—NH—CH_2—CH_2—$(CH_2)_7$—CH_3], 1.52 [—CO—NH—CH_2—C**H**$_2$—$(CH_2)_7$—CH_3], 1.32 [—CO—NH—CH_2—CH_2—(C**H**$_2$)$_7$—CH_3], 0.92 [—CO—NH—CH_2—CH_2—$(CH_2)_7$—C**H**$_3$]. FTIR (ν, cm^{-1}): 3286, 3074, 2960, 2926, 2852, 2815, 1740, 1650, 1550, 1465, 1359, 1259, 1195, 1126, 1042, 724.

PEO–PEI Dendritic Diblock Generation 2.0: Dodecyl-Terminated

Yellow, soft solid. Yield: 0.23 g, 61%. Substitution: 95%. ^{1}H NMR ($CDCl_3$): 3.68 (unreacted —CH_2—CH_2—CO—OC**H**$_3$), 3.66 (—O—C**H**$_2$—C**H**$_2$—), 3.33 (—CO—NH—C**H**$_2$—CH_2—N<), 3.18 [—CO—NH—C**H**$_2$—CH_2—$(CH_2)_9$—CH_3], 2.77 (—C**H**$_2$—CH_2—CO—NH—CH_2—CH_2—N<) and [—C**H**$_2$—CH_2—CO—NH—CH_2—CH_2—$(CH_2)_9$—CH_3], 2.55 (—N—C**H**$_2$—C**H**$_2$— and —CO—NH—CH_2—C**H**$_2$—N<), 2.36 (—CH_2—C**H**$_2$—CO—NH—CH_2—CH_2—N<) and [—CH_2—C**H**$_2$—CO—NH—CH_2—CH_2—$(CH_2)_9$—CH_3], 1.50 [—CO—NH—CH_2—C**H**$_2$—$(CH_2)_9$—CH_3], 1.27 [—CO—NH—CH_2—CH_2—(C**H**$_2$)$_9$—CH_3], 0.90 [—CO—NH—CH_2—CH_2—$(CH_2)_9$—C**H**$_3$]. FTIR (ν, cm^{-1}): 3287, 3073, 2963, 2924, 2848, 2815, 1739, 1640, 1552, 1465, 1360, 1256, 1102, 1026, 718.

PEO–PEI Dendritic Diblock Generation 2.0: Octadecyl-Terminated

Light yellow solid. Yield: 0.21 g, 63%. Substitution: 27%. ^{1}H NMR ($CDCl_3$): 3.68 (unreacted —CH_2—CH_2—CO—OC**H**$_3$), 3.66 (—O—C**H**$_2$—C**H**$_2$—), 3.31 (—CO—NH—C**H**$_2$—CH_2—N<), 3.18 [—CO—NH—C**H**$_2$—CH_2—$(CH_2)_{15}$—CH_3], 2.77 (—C**H**$_2$—CH_2—CO—NH—CH_2—CH_2—N<) and [—C**H**$_2$—CH_2—CO—NH—CH_2—CH_2—$(CH_2)_{15}$—CH_3], 2.56 (—N—C**H**$_2$—C**H**$_2$— and —CO—NH—CH_2—C**H**$_2$—N<), 2.45 (unreacted —CH_2—C**H**$_2$—CO—OCH_3), 2.37 (—CH_2—C**H**$_2$—CO—NH—CH_2—CH_2—N<) and [—CH_2—C**H**$_2$—CO—NH—CH_2—CH_2—$(CH_2)_{15}$—CH_3], 1.50 [—CO—NH—CH_2—C**H**$_2$—$(CH_2)_{15}$—CH_3], 1.27 [—CO—NH—CH_2—CH_2—(C**H**$_2$)$_{15}$—CH_3], 0.90 [—CO

—NH—CH_2—CH_2—$(CH_2)_{15}$—C**H$_3$**]. FTIR (ν, cm^{-1}): 3277, 3067, 2959, 2921, 2851, 2813, 1740, 1648, 1551, 1470, 1438, 1362, 1254, 1200, 1125, 1044, 758.

PEO–PEI Dendritic Diblock Generation 3.0: Butyl-Terminated

Clear, yellow solid. Yield: 0.27 g, 85%. Substitution: 99%. ^{1}H NMR (MeOH-*d*): 3.65 (—O—C**H$_2$**—C**H$_2$**—), 3.28 (—CO—NH—C**H$_2$**—CH_2—N<), 3.19 (—CO—NH—C**H$_2$**—CH_2—CH_2—CH_3), 2.84 (—C**H$_2$**—CH_2—CO—NH—CH_2—CH_2—N<), 2.81 (—C**H$_2$**—CH_2—CO—NH—CH_2—CH_2—CH_2—CH_3), 2.61 (—N—C**H$_2$**—C**H$_2$**— and —CO—NH—CH_2—C**H$_2$**—N<), 2.40 (—CH_2—C**H$_2$**—CO—NH—CH_2—CH_2—N<), 2.38 (—CH_2—C**H$_2$**—CO—NH—CH_2—CH_2—CH_2—CH_3), 1.50 (—CO—NH—CH_2—C**H$_2$**—CH_2—CH_3), 1.39 (—CO—NH—CH_2—CH_2—C**H$_2$**—CH_3), 0.96 (—CO—NH—CH_2—CH_2—CH_2—C**H$_3$**). FTIR (ν, cm^{-1}): 3285, 3077, 2960, 2933, 2869, 2821, 1640, 1552, 1466, 1365, 1247, 1151, 1039, 757.

PEO–PEI Dendritic Diblock Generation 3.0: Hexyl-Terminated

Clear, yellow solid. Yield: 0.28 g, 81%. Substitution: 97%. ^{1}H NMR (MeOH-*d*): 3.69 (unreacted —CH_2—CH_2—CO—OC**H$_3$**), 3.65 (—O—C**H$_2$**—C**H$_2$**—), 3.28 (—CO—NH—C**H$_2$**—CH_2—N<), 3.18 [—CO—NH—C**H$_2$**—CH_2—$(CH_2)_3$—CH_3], 2.84 (—C**H$_2$**—CH_2—CO—NH—CH_2—CH_2—N<), 2.81 [—C**H$_2$**—CH_2—CO—NH—CH_2—CH_2—$(CH_2)_3$—CH_3], 2.76 (unreacted —C**H$_2$**—CH_2—CO—OCH_3), 2.62 (—N—C**H$_2$**—C**H$_2$**— and —CO—NH—CH_2—C**H$_2$**—N<), 2.50 (unreacted —CH_2—C**H$_2$**—CO—OCH_3), 2.40 (—CH_2—C**H$_2$**—CO—NH—CH_2—CH_2—N<), 2.36 [—CH_2—C**H$_2$**—CO—NH—CH_2—CH_2—$(CH_2)_3$—CH_3], 1.52 [—CO—NH—CH_2—C**H$_2$**—$(CH_2)_3$—CH_3], 1.34 [—CO—NH—CH_2—CH_2—$(CH_2)_3$—CH_3], 0.93 [—CO—NH—CH_2—CH_2—$(CH_2)_3$—C**H$_3$**]. FTIR (ν, cm^{-1}): 3289, 3072, 2956, 2928, 2856, 2820, 1743, 1645, 1552, 1464, 1361, 1284, 1248, 1155, 1129, 1037, 732, 691.

PEO–PEI Dendritic Diblock Generation 3.0: Octyl-Terminated

Clear, yellow solid. Yield: 0.27 g, 80%. Substitution: 89%. ^{1}H NMR (MeOH-*d*): 3.69 (unreacted —CH_2—CH_2—CO—OC**H$_3$**), 3.65 (—O—C**H$_2$**—C**H$_2$**—), 3.28 (—CO—NH—C**H$_2$**—CH_2—N<), 3.18 [—CO—NH—C**H$_2$**—CH_2—$(CH_2)_5$—CH_3], 2.84 (—C**H$_2$**—CH_2—CO—NH—CH_2—CH_2—N<), 2.81 [—C**H$_2$**—CH_2—CO—NH—CH_2—CH_2—$(CH_2)_5$—CH_3], 2.76 (unreacted —C**H$_2$**—CH_2—CO—OCH_3), 2.61 (—N—C**H$_2$**—C**H$_2$**— and —CO—NH—CH_2—C**H$_2$**—N<), 2.50 (unreacted —CH_2—C**H$_2$**—CO—OCH_3), 2.40 (—CH_2—C**H$_2$**—CO—NH—CH_2—CH_2—N<), 2.36 [—CH_2—C**H$_2$**—CO—NH—CH_2—CH_2—$(CH_2)_5$—CH_3], 1.52 [—CO—NH—CH_2—C**H$_2$**—$(CH_2)_5$—CH_3], 1.34 [—CO—NH—CH_2—CH_2—$(CH_2)_5$—CH_3], 0.93 [—CO—NH—CH_2—CH_2—$(CH_2)_5$—C**H$_3$**]. FTIR (ν, cm^{-1}): 3289, 3072, 2959, 2923, 2856, 2820, 1743, 1640, 1547, 1464, 1372, 1284, 1248, 1155, 1134, 1037, 722.

PEO–PEI Dendritic Diblock Generation 3.0: Decyl-Terminated

Clear, yellow solid. Yield: 0.26 g, 82%. Substitution: 84%. ^{1}H NMR (MeOH-*d*): 3.69 (unreacted —CH_2—CH_2—CO—OC**H$_3$**), 3.65 (—O—C**H$_2$**—C**H$_2$**—), 3.28 (—CO—NH—C**H$_2$**—CH_2—N<), 3.18 [—CO—NH—C**H$_2$**—CH_2—$(CH_2)_7$—CH_3], 2.85 (—C**H$_2$**—CH_2—CO—NH—CH_2—CH_2—N<), 2.80 [—C**H$_2$**—CH_2—CO—NH—CH_2—CH_2—$(CH_2)_7$—CH_3], 2.76 (unreacted —C**H$_2$**—CH_2—CO—OCH_3), 2.63 (—N—C**H$_2$**—C**H$_2$**— and —CO—NH—CH_2—C**H$_2$**—N<), 2.50 (unreacted —CH_2—C**H$_2$**—CO—OCH_3), 2.40 (—CH_2—C**H$_2$**—CO—NH—CH_2—CH_2—N<), 2.36 [—CH_2—C**H$_2$**—CO—NH—CH_2—CH_2—$(CH_2)_7$—CH_3], 1.52 [—CO—NH—CH_2—C**H$_2$**—$(CH_2)_7$—CH_3], 1.32 [—CO—NH—CH_2—CH_2—$(CH_2)_7$—CH_3], 0.92 [—CO—NH—CH_2—CH_2—$(CH_2)_7$—C**H$_3$**]. FTIR (ν, cm^{-1}): 3285, 3073, 2956, 2923, 2856, 2815, 1737, 1644, 1551, 1463, 1359, 1256, 1199, 1152, 1132, 1049, 728.

PEO–PEI Dendritic Diblock Generation 3.0: Dodecyl-Terminated

Clear, yellow solid. Yield: 0.23 g, 75%. Substitution: 66%. ^{1}H NMR (MeOH-*d*): 3.69 (unreacted —CH_2—CH_2—CO—OC**H$_3$**), 3.65 (—O—C**H$_2$**—C**H$_2$**—), 3.28 (—CO—NH—C**H$_2$**—CH_2—N<), 3.18 [—CO—NH—C**H$_2$**—CH_2—$(CH_2)_9$—CH_3], 2.85 (—C**H$_2$**—CH_2—CO—NH—CH_2—CH_2—N<), 2.80 [—C**H$_2$**—CH_2—CO—NH—CH_2—CH_2—$(CH_2)_9$—CH_3], 2.76 (unreacted —C**H$_2$**—CH_2—CO—OCH_3), 2.62 (—N—C**H$_2$**—C**H$_2$**— and —CO—NH—CH_2—C**H$_2$**—N<), 2.51 (unreacted —CH_2—C**H$_2$**—CO—OCH_3), 2.40 (—CH_2—C**H$_2$**—CO—NH—CH_2—CH_2—N<), 2.36 [—CH_2—C**H$_2$**—CO—NH—CH_2—CH_2—$(CH_2)_9$—CH_3], 1.52 [—CO—NH—CH_2—C**H$_2$**—$(CH_2)_9$—CH_3], 1.31 [—CO—NH—CH_2—CH_2—$(CH_2)_9$—CH_3], 0.92 [—CO—NH—CH_2—CH_2—$(CH_2)_9$—C**H$_3$**]. FTIR (ν, cm^{-1}): 3285, 3078,

2965, 2923, 2856, 2815, 1743, 1649, 1551, 1463, 1359, 1256, 1199, 1152, 1124, 1044, 722.

PEO–PEI Dendritic Diblock Generation 3.0: Octadecyl-Terminated

Light yellow solid. Yield: 0.16 g, 56%. Substitution: 33%. ^{1}H NMR ($CDCl_3$): 3.69 (unreacted —CH_2—CH_2—CO—O**CH_3**), 3.67 (—O—**CH_2**—**CH_2**—), 3.29 (—CO—NH—**CH_2**—CH_2—N<), 3.20 [—CO—NH—**CH_2**—CH_2—$(CH_2)_{15}$—CH_3], 2.77 (—**CH_2**—CH_2—CO—NH—CH_2—CH_2—N<) and [—**CH_2**—CH_2—CO—NH—CH_2—CH_2—$(CH_2)_{15}$—CH_3], 2.56 (—N—**CH_2**—**CH_2**— and —CO—NH—CH_2—**CH_2**—N<), 2.45 (unreacted —CH_2—**CH_2**—CO—OCH_3), 2.38 (—CH_2—**CH_2**—CO—NH—CH_2—CH_2—N<) and [—CH_2—**CH_2**—CO—NH—CH_2—CH_2—$(CH_2)_{15}$—CH_3], 1.50 [—CO—NH—CH_2—**CH_2**—$(CH_2)_{15}$—CH_3], 1.27 [—CO—NH—CH_2—CH_2—(**CH_2**)$_{15}$—CH_3], 0.90 [—CO—NH—CH_2—CH_2—$(CH_2)_{15}$—**CH_3**]. FTIR (ν, cm^{-1}): 3284, 3069, 2961, 2919, 2849, 2817, 1736, 1645, 1549, 1469, 1437, 1362, 1260, 1201, 1153, 1132, 1046, 757, 725.

PEO–PEI Dendritic Diblock Generation 4.0: Butyl-Terminated

Clear, yellow solid. Yield: 0.27 g, 87%. Substitution: 99%. ^{1}H NMR (MeOH-*d*): 3.65 (—O—**CH_2**—**CH_2**—), 3.28 (—CO—NH—**CH_2**—CH_2—N<), 3.19 (—CO—NH—**CH_2**—CH_2—CH_2—CH_3), 2.81 (—**CH_2**—CH_2—CO—NH—CH_2—CH_2—N< and —**CH_2**—CH_2—CO—NH—CH_2—CH_2—CH_2—CH_3), 2.61 (—N—**CH_2**—**CH_2**— and —CO—NH—CH_2—**CH_2**—N<), 2.38 (—CH_2—**CH_2**—CO—NH—CH_2—CH_2—N< and —CH_2—**CH_2**—CO—NH—CH_2—CH_2—CH_2—CH_3), 1.49 (—CO—NH—CH_2—**CH_2**—CH_2—CH_3), 1.37 (—CO—NH—CH_2—CH_2—**CH_2**—CH_3), 0.96 (—CO—NH—CH_2—CH_2—CH_2—**CH_3**). FTIR (ν, cm^{-1}): 3283, 3074, 2956, 2930, 2871, 2817, 1645, 1554, 1463, 1437, 1356, 1233, 1153, 1041, 752, 693.

PEO–PEI Dendritic Diblock Generation 4.0: Hexyl-Terminated

Clear, yellow solid. Yield: 0.23 g, 71%. Substitution: 97%. ^{1}H NMR (MeOH-*d*): 3.69 (unreacted —CH_2—CH_2—CO—O**CH_3**), 3.65 (—O—**CH_2**—**CH_2**—), 3.28 (—CO—NH—**CH_2**—CH_2—N<), 3.18 [—CO—NH—**CH_2**—CH_2—$(CH_2)_3$—CH_3], 2.81 (—**CH_2**—CH_2—CO—NH—CH_2—CH_2—N<) and [—**CH_2**—CH_2—CO—NH—CH_2—CH_2—$(CH_2)_3$—CH_3], 2.76 (unreacted —**CH_2**—CH_2—CO—OCH_3), 2.62 (—N—**CH_2**—**CH_2**— and —CO—NH—CH_2—**CH_2**—N<), 2.50 (unreacted —CH_2—**CH_2**—CO—OCH_3), 2.38 (—CH_2—**CH_2**—CO—NH—CH_2—CH_2—N<) and [—CH_2—**CH_2**—CO—NH—CH_2—CH_2—$(CH_2)_3$—CH_3], 1.52 [—CO—NH—CH_2—**CH_2**—$(CH_2)_3$—CH_3], 1.34 [—CO—NH—CH_2—CH_2—(**CH_2**)$_3$—CH_3], 0.93 [—CO—NH—CH_2—CH_2—$(CH_2)_3$—**CH_3**]. FTIR (ν, cm^{-1}): 3283, 3075, 2960, 2927, 2855, 2818, 1739, 1646, 1548, 1460, 1436, 1367, 1247, 1197, 1152, 1131, 1039, 762, 688.

PEO–PEI Dendritic Diblock Generation 4.0: Octyl-Terminated

Clear, yellow solid. Yield: 0.28 g, 79%. Substitution: 94%. ^{1}H NMR (MeOH-*d*): 3.69 (unreacted —CH_2—CH_2—CO—O**CH_3**), 3.65 (—O—**CH_2**—**CH_2**—), 3.28 (—CO—NH—**CH_2**—CH_2—N<), 3.17 [—CO—NH—**CH_2**—CH_2—$(CH_2)_5$—CH_3], 2.82 (—**CH_2**—CH_2—CO—NH—CH_2—CH_2—N<) and [—**CH_2**—CH_2—CO—NH—CH_2—CH_2—$(CH_2)_5$—CH_3], 2.76 (unreacted —**CH_2**—CH_2—CO—OCH_3), 2.60 (—N—**CH_2**—**CH_2**— and —CO—NH—CH_2—**CH_2**—N<), 2.50 (unreacted —CH_2—**CH_2**—CO—OCH_3), 2.38 (—CH_2—**CH_2**—CO—NH—CH_2—CH_2—N<) and [—CH_2—**CH_2**—CO—NH—CH_2—CH_2—$(CH_2)_5$—CH_3], 1.52 [—CO—NH—CH_2—**CH_2**—$(CH_2)_5$—CH_3], 1.34 [—CO—NH—CH_2—CH_2—(**CH_2**)$_5$—CH_3], 0.92 [—CO—NH—CH_2—CH_2—$(CH_2)_5$—**CH_3**]. FTIR (ν, cm^{-1}): 3285, 3077, 2953, 2922, 2853, 2820, 1744, 1642, 1552, 1461, 1440, 1365, 1285, 1247, 1157, 1039, 724, 684.

PEO–PEI Dendritic Diblock Generation 4.0: Decyl-Terminated

Clear, yellow solid. Yield: 0.31 g, 80%. Substitution: 90%. ^{1}H NMR (MeOH-*d*): 3.69 (unreacted —CH_2—CH_2—CO—O**CH_3**), 3.65 (—O—**CH_2**—**CH_2**—), 3.28 (—CO—NH—**CH_2**—CH_2—N<), 3.18 [—CO—NH—**CH_2**—CH_2—$(CH_2)_7$—CH_3], 2.80 (—**CH_2**—CH_2—CO—NH—CH_2—CH_2—N<) and [—**CH_2**—CH_2—CO—NH—CH_2—CH_2—$(CH_2)_7$—CH_3], 2.60 (—N—**CH_2**—**CH_2**— and —CO—NH—CH_2—**CH_2**—N<), 2.50 (unreacted —CH_2—**CH_2**—CO—OCH_3), 2.36 (—CH_2—**CH_2**—CO—NH—CH_2—CH_2—N<) and [—CH_2—**CH_2**—CO—NH—CH_2—CH_2—$(CH_2)_7$—CH_3], 1.52 [—CO—NH—CH_2—**CH_2**—$(CH_2)_7$—CH_3], 1.32 [—CO—NH—CH_2—CH_2—(**CH_2**)$_7$—CH_3], 0.92 [—CO—NH—CH_2—CH_2—$(CH_2)_7$—**CH_3**]. FTIR (ν, cm^{-1}): 3288, 3074, 2959, 2925, 2854, 2818, 1739, 1645, 1550, 1467, 1440, 1362, 1289, 1252, 1200, 1153, 1037, 723.

PEO–PEI Dendritic Diblock Generation 4.0: Dodecyl-Terminated

Clear, yellow solid. Yield: 0.22 g, 50%. Substitution: 99%. ^{1}H NMR ($CDCl_3$): 3.66 (—O—C**H$_2$**—C**H$_2$**—), 3.25 (—CO—NH—C**H$_2$**—CH_2—N<), 3.18 [—CO—NH—C**H$_2$**—CH_2—$(CH_2)_9$—CH_3], 2.75 (—C**H$_2$**—CH_2—CO—NH—CH_2—CH_2—N<) and [—C**H$_2$**—CH_2—CO—NH—CH_2—CH_2—$(CH_2)_9$—CH_3], 2.54 (—N—C**H$_2$**—C**H$_2$**— and —CO—NH—CH_2—C**H$_2$**—N<), 2.36 (—CH_2—C**H$_2$**—CO—NH—CH_2—CH_2—N<) and [—CH_2—C**H$_2$**—CO—NH—CH_2—CH_2—$(CH_2)_9$—CH_3], 1.50 [—CO—NH—CH_2—C**H$_2$**—$(CH_2)_9$—CH_3], 1.27 [—CO—NH—CH_2—CH_2—(C**H$_2$**)$_9$—CH_3], 0.89 [—CO—NH—CH_2—CH_2—$(CH_2)_9$—C**H$_3$**]. FTIR (ν, cm^{-1}): 3285, 3078, 2961, 1931, 2855, 2814, 1740, 1648, 1552, 1471, 1436, 1375, 1263, 1035, 807, 726.

PEO–PEI Dendritic Diblock Generation 4.0: Octadecyl-Terminated

Yellow solid. Yield: 0.11 g, 49%. Substitution: 12%. ^{1}H NMR ($CDCl_3$): 3.69 (unreacted —CH_2—CH_2—CO—OC**H$_3$**), 3.66 (—O—C**H$_2$**—C**H$_2$**—), 3.29 (—CO—NH—C**H$_2$**—CH_2—N<), 2.77 (—C**H$_2$**—CH_2—CO—NH—CH_2—CH_2—N<) and [—C**H$_2$**—CH_2—CO—NH—CH_2—CH_2—$(CH_2)_{15}$—CH_3], 2.56 (—N—C**H$_2$**—C**H$_2$**— and —CO—NH—CH_2—C**H$_2$**—N<), 2.45 (unreacted —CH_2—C**H$_2$**—CO—OCH_3), 2.38 (—CH_2—C**H$_2$**—CO—NH—CH_2—CH_2—N<) and [—CH_2—C**H$_2$**—CO—NH—CH_2—CH_2—$(CH_2)_{15}$—CH_3], 1.50 [—CO—NH—CH_2—C**H$_2$**—$(CH_2)_{15}$—CH_3], 1.27 [—CO—NH—CH_2—CH_2—(C**H$_2$**)$_{15}$—CH_3], 0.90 [—CO—NH—CH_2—CH_2—$(CH_2)_{15}$—C**H$_3$**]. FTIR (ν, cm^{-1}): 3287, 3073, 2963, 2922, 2853, 2815, 1740, 1653, 1543, 1467, 1438, 1363, 1259, 1203, 1044, 755, 662.

Instrumentation for Chemical Structure Verification

NMR analysis was performed on a Bruker 400 (400-MHz) instrument with the solvents DMSO-d_6, $CDCl_3$, and MeOH-d_4 as indicated. FTIR spectra were collected on a Nicolet Magna IR 550 spectrometer from thin, solution-cast films of the polymers on KBr plates. Gel permeation chromatography (GPC) in tetrahydrofuran (THF) was performed on a Waters system through Styragel HT3 and HT4 columns. Size exclusion chromatography/multi-angle laser light scattering (SEC–MALLS) was performed with a 0.1 M citric acid buffer through two TosoHaas TSK gel columns in series (G6000PW and G4000PW) and one Waters Ultrahydrogel 250 column in our laboratory. The SEC–MALLS system consisted of a Waters model 150C, which was connected to a Wyatt Dawn model F multi-angle light scattering detector.

DSC

DSC measurements were recorded with a PerkinElmer DSC7 calorimeter equipped with a compressed air sample dry box and a PerkinElmer refrigerated cooling system. The 4–8-mg polymer samples were prepared in aluminum pans, and each sample was heated and cooled at a rate of 10 °C/min under nitrogen. For the detection of any major changes in material behavior upon an initial heat treatment, each sample was subjected to two heating/cooling cycles. The melting points (T_m's) and glass-transition temperatures (T_g's) were calculated from the first heating/cooling cycle because there were generally no differences between the results of the two cycles. T_g was calculated with the half-height method, which used the midpoint of the inflection tangent. T_m was calculated on the basis of the mean of the area under T_m.

SAXS

Small-angle X-ray experiments were performed *in vacuo* with a Siemens computer-controlled system with a rotating anode that produced Cu Kα radiation (λ = 1.54 Å) at 40 kV and 30 mA. Samples for analysis were prepared through the dissolution of the polymers in a minimum of the solvent and the casting of the polymer solutions onto glass slides coated with Teflon tape. The glass slides were then placed under a crystallization dish along with a small beaker of the casting solvent to maintain equilibrium during the evaporation process. After 2 days, the majority of the casting solvent had evaporated. All the polymer samples were cast from methanol, except for the generation 4.0 dodecyl polymer, which was cast from chloroform, as this polymer was not completely soluble in methanol. The samples were then placed in a vacuum oven and annealed *in vacuo* for a minimum of 2 days at a temperature just below the highest T_m (between 37 and 53 °C). The cast films were carefully transferred to thin-walled glass capillary tubes, which were used in the SAXS instrument. The filled capillary tubes were then placed in a custom-built copper sample holder, which fit into an Instec model HS250 hot

stage (modified for vacuum operation), so that the samples were suspended vertically in the beam's path, 63.4 cm away from the detector. An Instec model STC200 temperature controller was used to control the temperature of the samples. Data were collected at various temperatures, starting at room temperature and increasing incrementally, usually in 5–10 °C intervals, until the temperature at which the last transition was observed in DSC was surpassed. The data were acquired with a detector consisting of a pressurized xenon chamber with a wire grid assembly that enabled direct imaging of the diffraction patterns, and the scattered X-ray intensity was plotted as a function of the temperature and scattering vector $\mathbf{q}$ [$\mathbf{q} = (4\pi \sin \theta)/\lambda$, where θ is one-half of the scattering angle].

TEM

TEM images were captured on JEOL JEM 2000 FX and JEOL JEM 2010 electron microscopes. For consistency, polymer samples for both TEM and SAXS were taken from the same cast film; therefore, the conditions for the polymer sample preparation were identical to those described for the SAXS experiments. Ultrathin films were prepared through the cryotoming of the polymer samples at −40 °C with an RMC MTX microtome with a diamond knife. Sections were transferred dry from the diamond knife surface onto copper grids and then stained for 60 min with RuO_4 vapor, which selectively stained the PAMAM regions dark, to provide contrast for electron imaging.

RESULTS AND DISCUSSION

Synthesis and Structural Characterization

The target linear–dendritic rod diblock copolymers consisted of a linear PEO–LPEI (PEO–PEI) diblock copolymer to which PAMAM branches were divergently added to the PEI block. The PEO linear block was chosen to achieve a water-soluble anchoring block for studies of the amphiphilic properties and the construction of films with Langmuir–Blodgett techniques, which will be addressed in a separate article. PEO, which exhibits a low T_g and is crystallizable, is also soluble in many organic solvents and is available as a block with low polydispersity in a number of different molecular weights. The PAMAM dendrimer chemistry was chosen for its ease of synthesis and functionalizable terminal amino groups. The end-functional groups of the dendritic branches are amine and ester groups formed during the generational synthesis; however, the ester groups can also be easily converted into alkyl groups of various lengths to introduce hydrophobicity in the dendritic block and thus induce the amphiphilic nature of the diblock copolymer. The development of a method for dendritic end-group functionalization that maintained the exact branch chemistry and that was applicable over several generations as well as a wide range of lengths of alkyl groups was desired.

For the synthesis of the PAMAM dendritic rod block, the PAMAM branches were synthesized in the same manner as spherical dendrimers[53,54] by the divergent building of the branches outward by the alternating addition of methyl acrylate and ethylenediamine, but from an LPEI core; this resulted in a branch extending from each repeat unit of the polymer. Because PEO was known to be soluble in methanol[55] and stable in the presence of ethylenediamine and methyl acrylate,[32] we could apply the same PAMAM reactions to a PEO–PEI backbone, without any side reactions. We found the optimal method for the synthesis of the desired PEO–PEI backbone to be a two-step PEO–tosylate macroinitiator approach. In this approach, PEO–tosylate was used as a macroinitiator in the cationic ring-opening polymerization of 2-ethyl-2-oxazoline (PEOX); this formed an intermediate PEO–PEOX diblock copolymer, which was then hydrolyzed to form the desired PEO–PEI diblock copolymer backbone,[52] as depicted in Figure 2(a).

Harris et al.[51] developed a method for PEO tosylation using triethylamine as the base, and this method was applied successfully to form the PEO–tosylate macroinitiator. From the ^{1}H NMR analysis of the PEO–tosylate products, we found that the tosylation was close to quantitative. In addition, GPC of both series of polymers in THF before and after tosylation indicated no breakdown of the PEO block in the presence of triethyl ammonium chloride salt byproducts. The polymerization of 2-ethyl-2-oxazoline,[56] as well as other 2-substituted oxazolines,[52,57,58] with a PEO–tosylate macroinitiator has been successfully described in the literature. The procedure used here is described schematically in Figure 2(a). The pseudo-controlled cationic ring-opening polymerization of oxazoline was used to create a PEO–PEOX diblock copolymer; from SEC, the

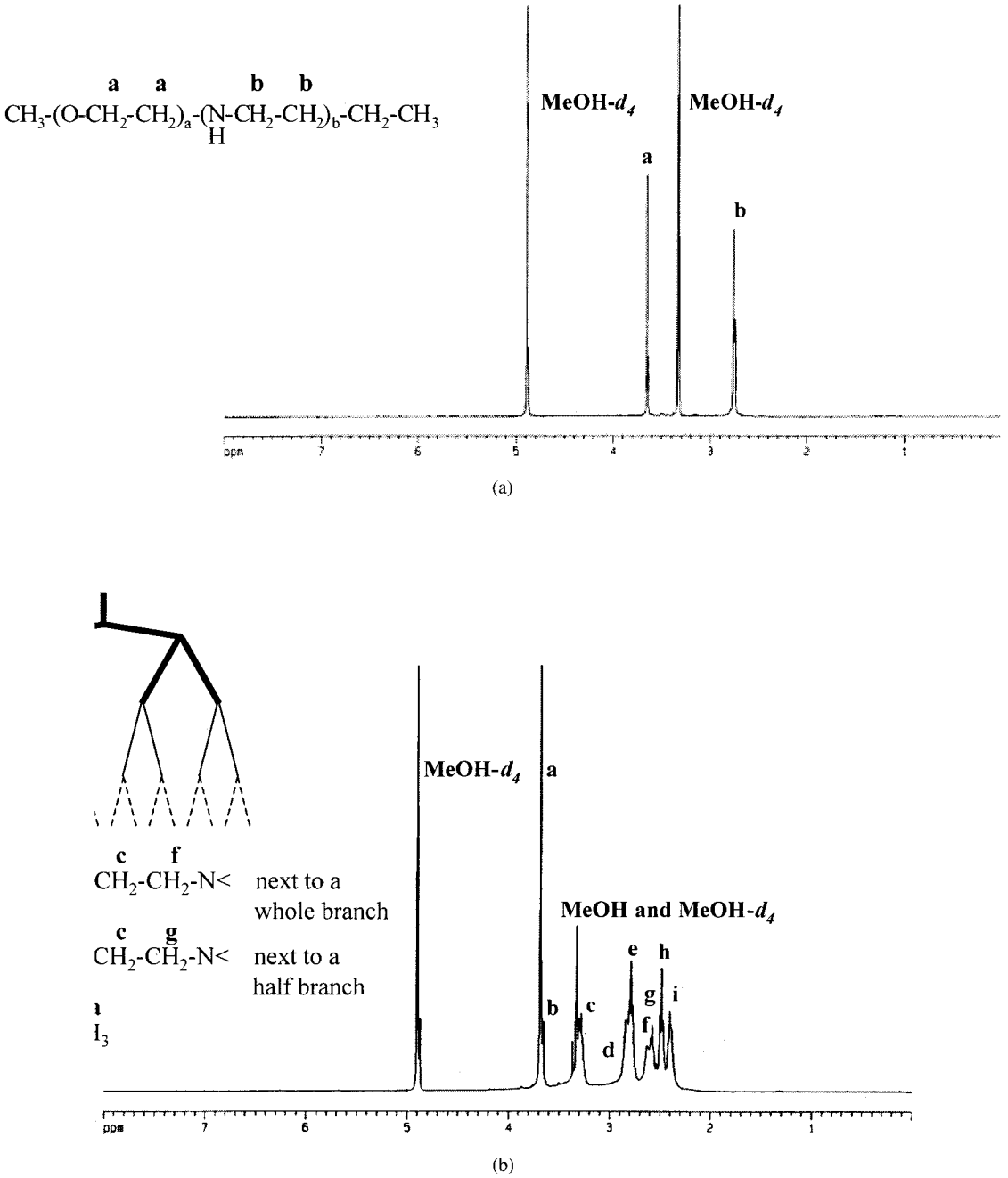

Figure 4. ^{1}H NMR spectra of (a) the PEO–PEI diblock copolymer consisting of 43 repeats of PEO and 97 repeats of PEI and (b) the generation 4.5 linear–dendritic rod diblock copolymer.

polydispersity of the diblock copolymer was found to be approximately 1.2, and the structures of both blocks were verified with NMR and FTIR. The hydrolysis of the PEO–PEOX diblock copolymer into the PEO–LPEI diblock copolymer was accomplished with a weak acid. ^{1}H NMR showed that approximately 100% of the amide groups were hydrolyzed [Fig. 4(a)]. The peak due to the PEOX main chain at 3.47 ppm disappeared and was replaced by a peak at 2.75 ppm due to the PEI main chain, whereas the peak due to the PEO protons remained virtually unchanged at 3.65 ppm. The proton on the secondary amine of the PEI block was not observed in ^{1}H NMR because of

the exchange of the proton with the deuterated methanol, as observed for PEI homopolymers.[59] The length of the PEI block was determined by the integration of the protons associated with each of the blocks. For the linear–dendritic rod diblock copolymers described here, the PEO block had a length of approximately 43 repeats, and the PEI dendritic block had a length of approximately 97 repeats.

The formation of the methyl ester terminated half-generation polymers proceeded as expected with the addition of methyl acrylate to the PEO–LPEI diblock copolymer backbone or amino-terminated branched polymer. As the generation number increased, so did the molar excess of methyl acrylate; for example, for the generation 1.5 diblock copolymer, a molar excess of 4.7 was employed, whereas for the generation 4.5 diblock copolymer, a molar excess of 7.6 was used. The structures of all the half-generation, methyl ester terminated polymers were confirmed with ^{1}H NMR and FTIR. The chemical structure of these polymers was confirmed by peaks at 3.69 (—CH_2—CH_2—CO—O**C**$\mathbf{H_3}$), 2.85 (—**C**$\mathbf{H_2}$—CH_2—CO—OCH_3), and 2.53 (—CH_2—**C**$\mathbf{H_2}$—CO—OCH_3), as well as a shift in the PEI backbone protons to 2.61 ppm (—N—**C**$\mathbf{H_2}$—**C**$\mathbf{H_2}$—). The PEO peak remained unchanged at 3.65 ppm. A representative NMR spectrum of the generation 4.5 polymer is shown in Figure 4(b). The set of ratios of the peaks due to the exterior branches (—**C**$\mathbf{H_2}$—**C**$\mathbf{H_2}$—CO—O**C**$\mathbf{H_3}$) to the peaks due to the interior branches (—**C**$\mathbf{H_2}$—**C**$\mathbf{H_2}$—CO—NH—**C**$\mathbf{H_2}$—**C**$\mathbf{H_2}$—N<) were found to decrease as the generation increased, as expected. For example, for the generation 1.5 polymers, the ratio was 2:1 = 2, whereas for the generation 3.5 polymers, the ratio was 8:7 = 1.14.

The reaction of the methyl ester terminated polymers with ethylenediamine to form the whole-generation, amine-terminated polymers required huge excesses of ethylenediamine [Fig. 2(b)], at low temperatures (ca. 5 °C), for long times to prevent the polymer from intermolecular and intramolecular crosslinking. The ^{1}H NMR spectra of all the amine-terminated polymers possessed all the same peaks because the branch chemistry remained identical as the generation increased. The integration of the NMR peaks for both the half- and whole-generation polymers, as well as a complete disappearance of the methyl ester protons at 3.69 ppm during the formation of the whole-generation polymers, indicated that close to 100% substitution occurred at each generation. The proton of the amide group did not appear in the spectra for either the half- or whole-generation polymers because of the exchange of the proton with the deuterated methanol. The peak positions for both the amine and methyl ester terminated polymers were in good agreement with those found for the PAMAM spherical[53,54,60,61] and hybrid linear–dendritic diblock copolymers.[32]

To make the diblock copolymers amphiphilic, we functionalized the end groups of the dendritic block with butyl-to-dodecyl alkyl chains. We accomplished this by reacting the methyl ester terminated, half-generation polymers with the *n*-alkyl amines, and this resulted in the amidation of the methyl ester groups and the formation of terminal alkyl groups. To accelerate the reaction and achieve high degrees of substitution of the alkyl groups on the chain ends, we used large excesses, approximately 60 times for the butyl amine reactions to approximately 20–30 times for the dodecyl amine reactions. In addition, the reaction solutions were heated to 40–50 °C. Functionalization with octadecyl groups was hindered by kinetics because of the crystalline nature of the octadecyl groups (and the octadecyl amine used in the alkylation reaction); these polymers were substituted at low degrees of substitution ranging from 12 to 33%. The resulting systems were highly amphiphilic, despite low substitution levels; the results from these polymers will not be addressed here for that reason.

The addition of the alkyl groups was confirmed by the addition of NMR peaks at approximately 3.20 [—CO—NH—C**H**$_2$—CH_2—$(CH_2)_{n-3}$—CH_3], 1.51 [—CO—NH—CH_2—C**H**$_2$—$(CH_2)_{n-3}$—CH_3], 1.38 [—CO—NH—CH_2—CH_2—(C**H**$_2$)$_{n-3}$—CH_3], and 0.94 ppm [—CO—NH—CH_2—CH_2—$(CH_2)_{n-3}$—C**H**$_3$], all from the alkyl protons. As an example, the spectrum of the generation 3.0 octyl-terminated polymer, which is very representative of the alkyl-terminated polymers, is provided in Figure 5. Unfortunately, for most of the polymers, not all the methyl ester groups reacted to full conversion, as indicated by residual protons at 3.69 (—CH_2—CH_2—CO—O**C**$\mathbf{H_3}$), 2.76 (—**C**$\mathbf{H_2}$—CH_2—CO—OCH_3), and 2.50 ppm (—CH_2—**C**$\mathbf{H_2}$—CO—OCH_3). ^{1}H NMR was used to determine the substitution percentage of the *n*-alkyl amines on the ester-terminated polymers through a comparison of the integration values of peaks attributed to functionalized and nonfunctionalized repeat units. Specifically, the integration value from the nonfunctionalized methyl ester

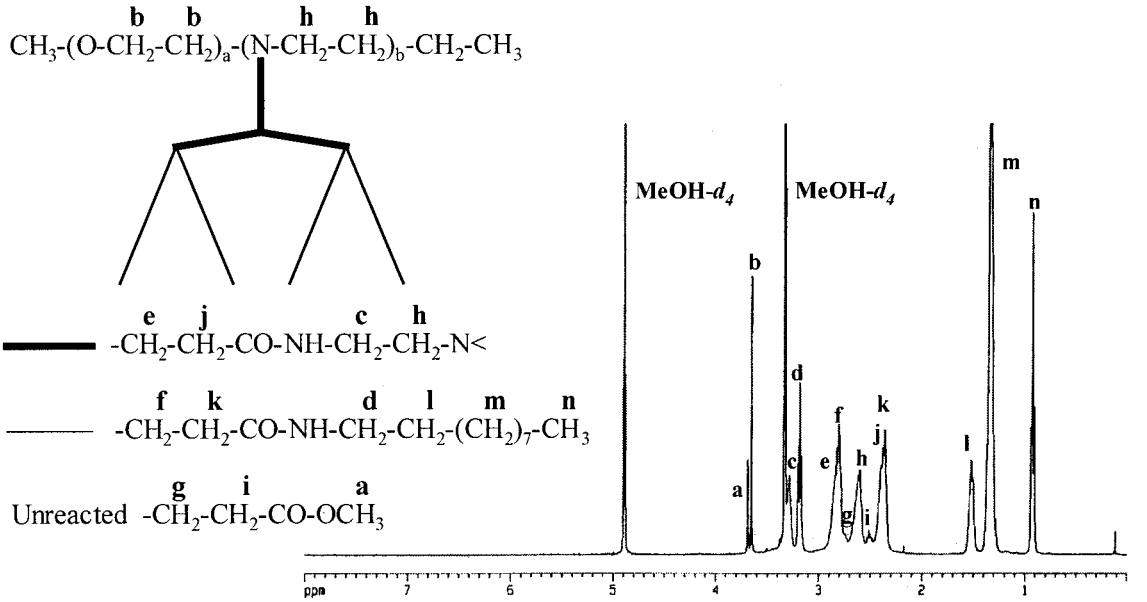

Figure 5. ^{1}H NMR spectrum of the generation 3.0 octyl-terminated linear–dendritic rod diblock copolymer.

group (—CH_2—CH_2—CO—O**CH_3**), which appeared around 3.69 ppm, was compared to the integration values from the CH_2 adjacent to the newly formed amide group [—CO—NH—**CH_2**—CH_2—$(CH_2)_n$—CH_3], which appeared at 3.18 ppm, and the terminal methyl group of the alkyl chain [—CO—NH—CH_2—CH_2—$(CH_2)_{n-3}$—**CH_3**], which appeared at 0.92 ppm. For each alkyl-substituted system, the polymer, its substitution percentage, its molecular weight, and its PEO are listed in Table 1. FTIR was also used to verify the chemical structures of all the linear–dendritic rod diblock copolymers synthesized through the identification of the functional groups present; all findings further confirmed the synthesis of the diblock backbone and the successful growth of the dendritic branches along the polymer backbone, as well as subsequent alkyl substitution.

Attempts were made to characterize the PEO–PEOX and PEO–LPEI diblock copolymers by matrix-assisted laser desorption/ionization time-of-flight (MALDI-TOF). Unfortunately, these polymers did not meet the stringent monodispersity requirements for MALDI-TOF and therefore did not yield meaningful results. Furthermore, molecular weight characterization with SEC–MALLS was also not possible; reproducible results could not be obtained for these linear–dendritic rod diblock copolymers, despite careful attempts, because of the binding of the polymer to the column, as well as the partially charged and highly branched nature of the polymers in solution. Similar difficulties were reported for dendritic rod systems by Percec et al.[12] and for other highly branched polymers.[62–64] For these reasons, NMR remained the best means of determining the molecular weight of each species, as previously described.

Thermal Behavior

One of the thermal transitions that has been extensively studied in dendritic systems is T_g. Researchers have been interested in how T_g is affected by the generation number, interior chemistry, and exterior functionality of a dendrimer. As these studies have extended to the thermal properties in hybrid linear–dendritic diblock copolymer systems, many of which possess a linear block that is semicrystalline, the effects of the dendrimer generation number and chemistry on T_m of the linear block have also been examined. Thus, given the unique chemistry and architecture of the PEO–LPEI linear–dendritic rod diblock copolymers, the thermal transitions of the polymers were examined to determine the effects of the dendritic block generation and exterior chemistry on T_g and T_m of the polymers.

The thermal transitions of each of the linear–dendritic rod diblock copolymers were measured

Table 1. Summary of the Synthesized Polymers, the Substitution Percentages of the Terminal Groups, the Resulting Molecular Weights as Calculated by ^{1}H NMR, and the Weight Percentages of PEO

Generation	End Group	Substitution (%)	Molecular Weight (g/mol)	PEO (wt %)
PEO–PEI			6100	31%
PEO–PEI generation 0.5	Methyl ester	100%	14,500	13%
PEO–PEI generation 1.0	Amine	100%	17,200	11%
	Butyl	98%	18,400	10%
	Hexyl	95%	20,800	9.1%
	Octyl	87%	22,600	8.4%
	Decyl	93%	25,700	7.3%
	Dodecyl	90%	27,800	6.8%
PEO–PEI generation 1.5	Methyl ester	100%	33,900	5.6%
PEO–PEI generation 2.0	Amine	100%	39,300	4.8%
	Butyl	82%	40,400	4.7%
	Hexyl	98%	47,000	4.0%
	Octyl	96%	51,900	3.7%
	Decyl	76%	52,300	3.6%
	Dodecyl	95%	62,000	3.1%
PEO–PEI generation 2.5	Methyl ester	100%	72,600	2.5%
PEO–PEI generation 3.0	Amine	100%	83,500	2.3%
	Butyl	99%	88,400	2.1%
	Hexyl	97%	98,600	1.9%
	Octyl	89%	106,000	1.8%
	Decyl	84%	113,000	1.7%
	Dodecyl	66%	112,000	1.7%
PEO–PEI generation 3.5	Methyl ester	100%	150,000	1.3%
PEO–PEI generation 4.0	Amine	100%	172,000	1.1%
	Butyl	99%	182,000	1.0%
	Hexyl	97%	202,000	0.94%
	Octyl	94%	222,000	0.86%
	Decyl	90%	238,000	0.80%
	Dodecyl	99%	268,000	0.71%
PEO–PEI generation 4.5	Methyl ester	100%	305,000	0.62%

with DSC, and examples of traces for the PEO–LPEI backbone polymer as well as the generation 2.0 amine-terminated and generation 3.5 ester-terminated linear–dendritic rod diblock copolymers are presented in Figure 6.

The PEO–LPEI diblock copolymer consisted of two crystalline blocks, each block exhibiting more than one T_m. The T_m's for the PEO block were 30.6 and 38.6 °C, whereas those for the PEI block were 67.6 and 76.0 °C. T_m of pure PEO with a molecular weight of 2000 g/mol is known to be approximately 54 °C.[32] Thus, the presence of the PEI block resulted in a reduction of the PEO T_m, most likely because of a combination of destabilization of PEO crystals and phase mixing of the PEO and PEI blocks. The formation of two T_m's indicated that two different crystal structures were present, perhaps one in which the PEO block cocrystallized with or was plasticized by the PEI block, this resulting in a lower T_m, and one in which PEO was more fully segregated from the PEI block, this resulting in a slightly higher T_m. Another likely possibility is the formation of a population of smaller, less stable crystallites in the sample that melted at lower temperatures. Iyer et al.[32] also observed a reduction in T_m of the PEO block in PEO–PAMAM hybrid linear–dendritic diblock copolymer systems. In these systems, T_m decreased as the generation increased, so that its value was approximately 40 °C for the generation 4.0 amine-terminated polymer. Similarly, two different T_m's were observed that could be attributed to the PEI block of the PEO–LPEI diblock copolymer. The LPEI homopolymer is known to exhibit two different T_m's depending on the degree of hydration of the polymer. The an-

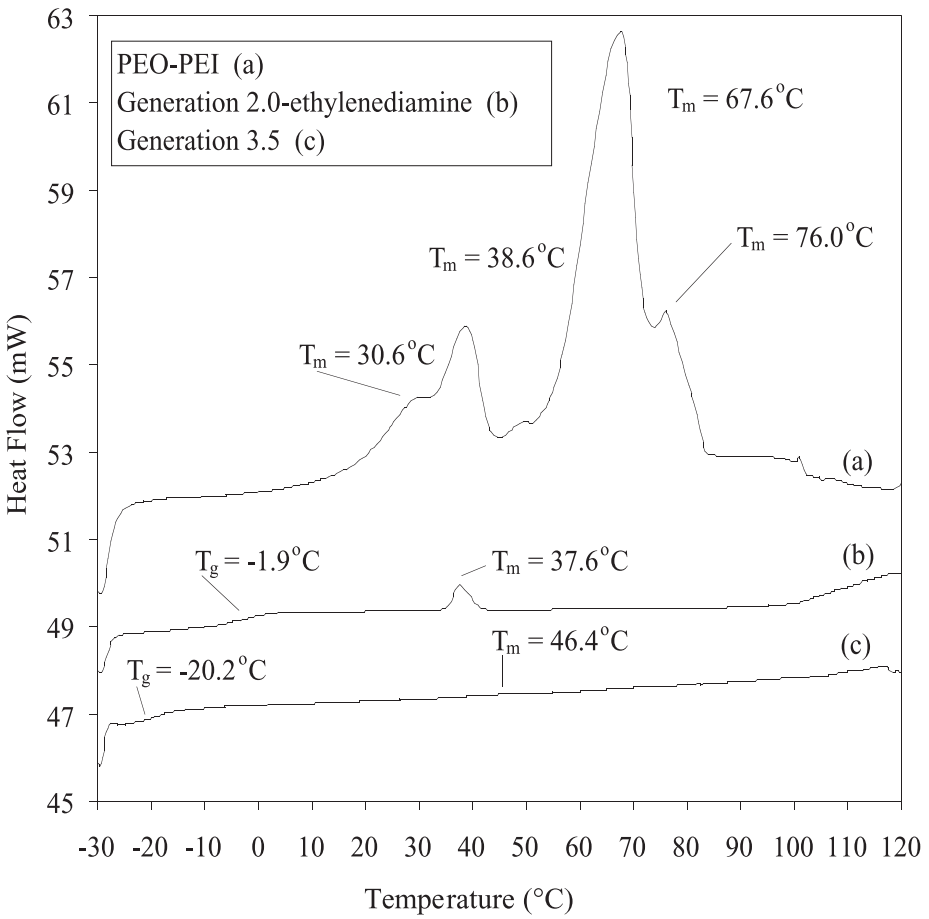

Figure 6. Examples of the first heating DSC traces for the amine- and ester-terminated linear–dendritic rod diblock copolymers: the PEO–PEI diblock copolymer backbone, the generation 2.0 linear–dendritic rod diblock copolymer, and the generation 3.5 linear–dendritic rod diblock copolymer.

hydrous polymer has a T_m of 58.5 °C, whereas the hydrated polymer has a T_m of 78.5 °C.[59,65,66] Thus, for the PEO–LPEI diblock copolymer, the T_m at 76.0 °C can be attributed to hydrated PEI. The T_m at 67.6 °C is fairly broad; thus, it can be attributed to a combination of PEI, which is anhydrous or only partially hydrated, and PEI, which has cocrystallized with the PEO block. Unfortunately, no T_g's were detected for the PEO–LPEI diblock copolymer because of limitations in the detection range of the equipment. T_g of the PEO block is known to be approximately −51 °C,[67] whereas that of the PEI block has been found to be approximately −25 °C.[66,68]

The addition of dendritic branches to the PEI block resulted in a loss of crystallinity of this block for the amine- and ester-terminated diblock copolymers formed during the generational synthesis; thus, these linear–dendritic rod diblock copolymers appeared to consist of an amorphous PAMAM dendritic block and a crystalline PEO block. T_m of the PEO block and T_g of the dendritic block have been plotted in Figure 7 as a function of the generation. T_m of the PEO block remained constant, at approximately 40 °C, being independent of the generation, and virtually disappeared above generation 2.0. This is not surprising because as the generation number increased, the weight fraction of PEO decreased, so that by generation 2.5, the weight fraction of PEO in the diblock copolymer was approximately 2.5%. In general, the PEO crystals observed at very low generations most likely consisted of PEO plasticized by the dendritic block, as indicated by a lowering of T_m of the PEO block to approximately 40 °C from that of approximately 54 °C for the PEO homopolymer and as observed for the PEO–LPEI diblock copolymer.

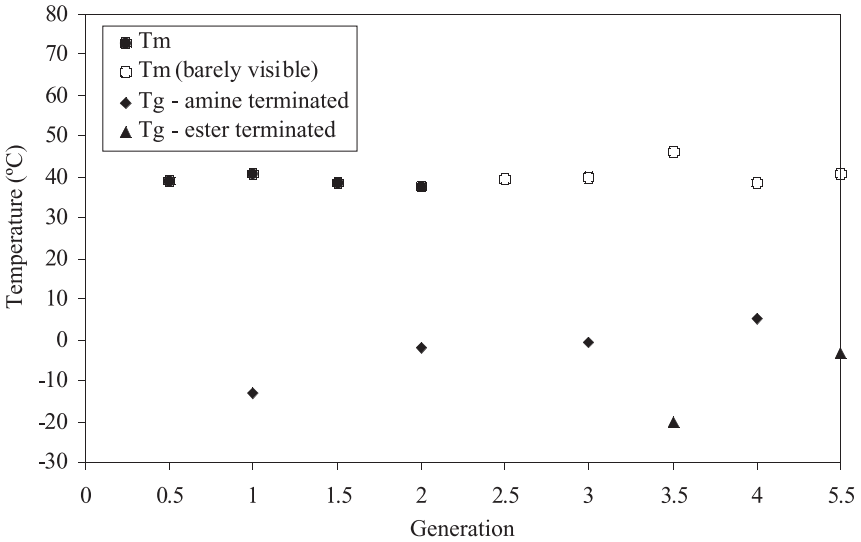

Figure 7. Variation of T_m and T_g with the generation for the amine- and ester-terminated linear–dendritic rod diblock copolymers.

A T_g attributed to the dendritic block was observed for all the amine-terminated polymers, as shown in Figure 7; however, it was only observed for the generation 3.5 and 4.5 ester-terminated polymers. The value of this T_g was always higher for the more polar amine-terminated polymers than for the ester-terminated polymers of the same degree of branching, most likely because of the stronger interactions between the more polar groups, which inhibited segmental motion. In addition, this T_g increased as the generation increased, most likely because of the increased stiffness of the branches, as well as the increased size of the dendrimer and thus the dispersive forces between the dendrimers, which also would have increased the energy necessary for segmental motion. Thus, the reason that a T_g was not observed for the low-generation methyl ester terminated polymers was most likely that it fell below the range of the detector. This dependence of T_g of the dendrimer on the dendrimer end-group chemistry and generation number has been observed for several other dendritic systems. Wooley et al.[69] first observed this behavior for poly(benzyl ether) dendrimers. Dendrimers that were terminated with cyano groups exhibited a higher T_g than those that were terminated with less polar benzyl groups. They also found that T_g increased with increasing molecular weight up to a point and then leveled off as the polymers became more globular and did not have as many opportunities for interdigitation. Similar results have been reported for cyano- and amine-terminated poly(propylene imine) dendrimers and for hyperbranched polyesters.[70,71] These trends were also observed in hybrid linear–dendritic diblock copolymer systems by Iyer et al.,[32] who observed a T_g for amine-terminated PEO–PAMAM hybrid linear–dendritic diblock copolymers that was 30 °C higher than that of the ester-terminated polymers of the same degree of branching. In addition, they found that T_g increased with increasing generation. These observations were theoretically predicted by Stutz[72] as well. Finally, the T_g's measured for the dendritic block of the amine and methyl ester terminated linear–dendritic rod diblock copolymer were in good agreement with those measured for other PAMAM dendritic systems.[32,73]

The functionalization of the dendritic block terminal branches with alkyl groups in the linear–dendritic rod diblock copolymers added crystallinity to the dendritic block, as indicated by the addition of an alkyl chain T_m at approximately 20 °C to the thermal transitions of these polymers. These functionalized polymers also maintained the dendritic block T_g and PEO T_m that had been observed in the unfunctionalized polymers. The thermal transitions of each of these alkylated linear–dendritic rod diblock copolymers were measured with DSC, and sample DSC traces illustrating these three transitions are shown in Figure 8. The four sample traces are for the generation 1.0 butyl, 3.0 butyl, 4.0 butyl, and 4.0 decyl linear–dendritic rod diblock copolymers. For these alkyl-terminated linear–dendritic rod diblock copolymers, T_m of the PEO block remained approxi-

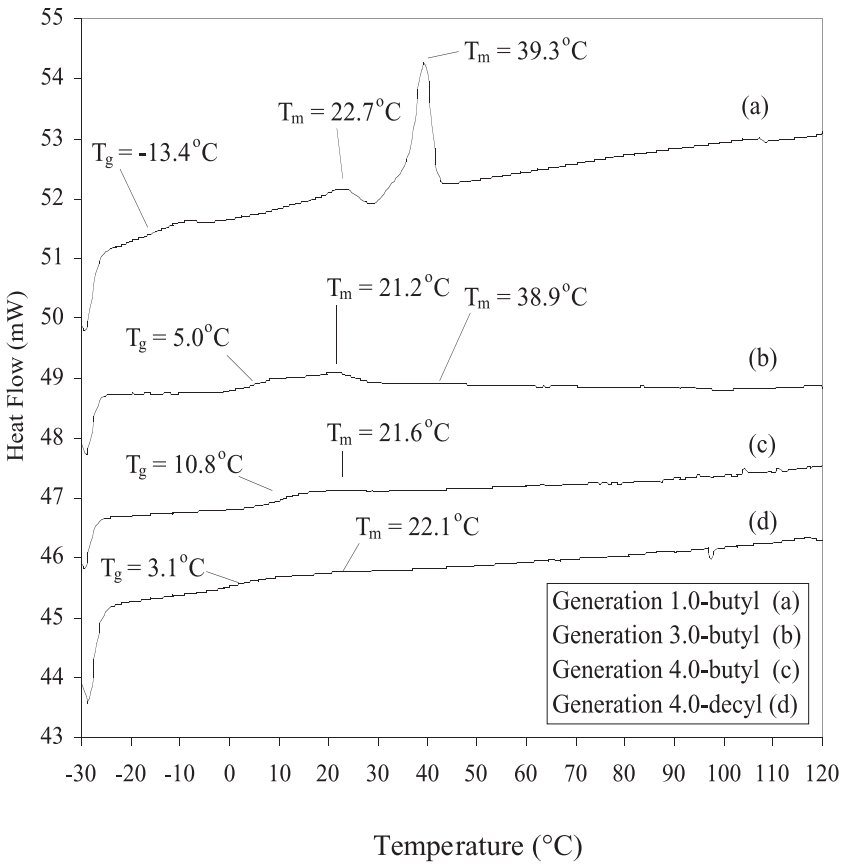

Figure 8. Examples of the first heating DSC traces for the alkyl-terminated linear–dendritic rod diblock copolymers: the generation 1.0 butyl-terminated linear–dendritic rod diblock copolymer, the generation 3.0 butyl-terminated linear–dendritic rod diblock copolymer, the generation 4.0 butyl-terminated linear–dendritic rod diblock copolymer, and the generation 4.0 decyl-terminated linear–dendritic rod diblock copolymer.

mately constant, being independent of the alkyl chain length and generation; this suggested a relatively unchanged degree of phase separation for the PEO block upon alkyl addition. In addition, T_m all but disappeared above generation two, and this indicated the complete loss of PEO crystallinity as the dendritic rod block increased in size and reflected a diminishing fraction of the polymer that consisted of PEO, as found with the methyl ester terminated and amine-terminated polymers.

An examination of Figure 8 also reveals the general trend that, as the generation increased, the relative enthalpy of melting for the alkyl chains decreased. Unlike the PEO block, the relative number of alkyl chains increased with increasing generation; thus, the decrease in the crystallinity could not be attributed to the number of alkyl groups present. Most likely, this decrease in the intensity was caused by the increased difficulty that the alkyl chains experienced trying to crystallize, as the dendritic interior became more congested and less able to adopt the conformations necessary for crystallization. As previously mentioned, Iyer and Hammond[39] also observed disorganization of the alkyl chains in their fourth-generation stearate-terminated linear–dendritic diblock copolymers due to the highly branched interior, which prevented alignment of the alkyl groups. T_m of the alkyl chains was found to be independent of the generation and was approximately constant for the butyl-to-dodecyl-terminated polymers. The constant alkyl chain T_m observed for the polymers terminated with the butyl-to-dodecyl groups was somewhat surprising, as the alkyl chain T_m is usually found to be very dependent on the alkyl chain length, increasing with increasing length.[74] Wei et al.[75] also observed an alkyl chain T_m that was independent of the alkyl chain length for semi-

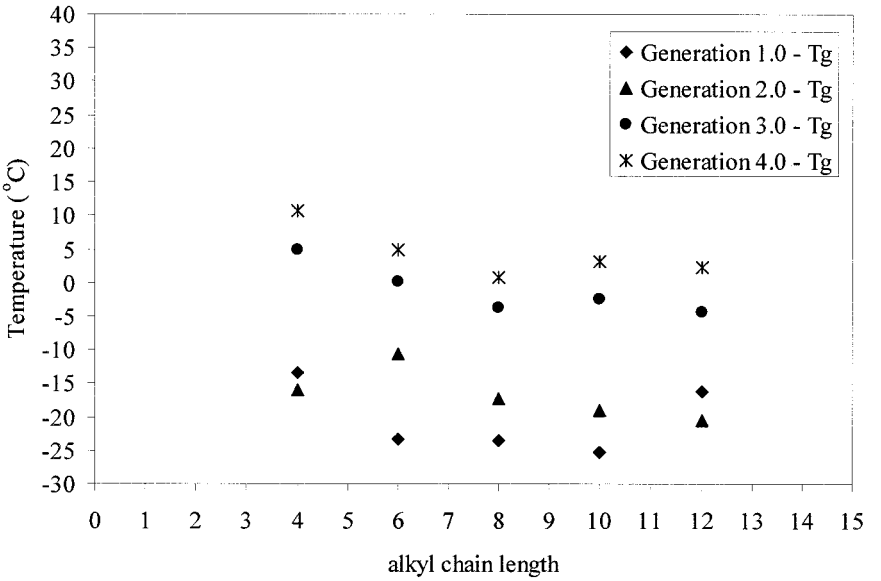

Figure 9. Variation of T_g with the alkyl chain length and generation for the alkyl-terminated linear–dendritic rod diblock copolymers.

crystalline poly(ether amine) dendrimers that had been terminated with myristoyl, palmitoyl, and octadecyl groups.

The T_g's of the alkyl-terminated polymers are summarized in Figure 9, which plots the dendritic T_g as a function of the alkyl chain length and dendrimer generation. As observed for the methyl ester terminated and amine-terminated linear–dendritic rod diblock copolymers, T_g of the alkyl-terminated diblock copolymers was dependent not only on the generation number of the dendritic block but also on its end-group chemistry or, more specifically for the alkyl-terminated polymers, on the length of the alkyl chain. In general, T_g of the dendritic block increased with increasing generation, and this was the same trend observed for the amine- and ester-terminated polymers. A general trend of decreasing T_g with increasing alkyl chain length was observed for all the dendritic rod polymers, as previously observed for the well-known poly(*n*-alkyl acrylate) series and for hyperbranched polyesters and aromatic poly(ether imide)s end-capped with various alkyl groups;[76,77] this effect is due to the internal plasticization of the long alkyl chains.[78]

For the generation 1.0 alkyl-terminated polymers, T_g decreased from approximately −13.4 °C for the generation 1.0 butyl-terminated polymer to −25.3 °C for the generation 1.0 decyl-terminated polymer; however, it then increased to −16.2 °C for the generation 1.0 dodecyl polymer. In general, polymers terminated with alkyl chains that possess 12 or more carbons have a higher degree of crystallinity than those possessing fewer than 12 carbons. Thus, the alkyl chains in the dodecyl-terminated generation 1.0 polymer were probably more highly crystalline and thus more effective in inhibiting the motion of the underlying branches than those terminated with the shorter alkyl chains. Wei et al.[75] found this to be the case when they examined semicrystalline dendritic polymers formed from second-generation poly(ether amine) dendrimers that had been functionalized with myristoyl, palmitoyl, and octadecyl groups. As the length of the alkyl chain increased, so did T_g as the introduction of longer alkyl chains increased the tendency for crystallization and the crystalline moiety forced the amorphous core into a more rigid structure. This upturn in T_g at a very high alkyl chain length was not observed for the higher generation polymers; it is likely that the more highly branched polymers did not accommodate the same high levels of crystallinity as that exhibited in generation 1.0.

For the generation 2.0 alkyl-terminated linear–dendritic rod diblock copolymers, the same trend of decreasing T_g with increasing alkyl chain length was observed. However, in this case, the generation 2.0 dodecyl polymer also exhibited a T_g that decreased in comparison with the generation 2.0 decyl-terminated polymer. As mentioned earlier, it is likely that the more highly

branched polymers reduced the ability of the dodecyl chains to crystallize and thus reduced the effect of the alkyl chains on T_g. Although T_g did decrease with increasing alkyl chain length, the magnitude of the decrease was not as large for the decyl and dodecyl polymers as it was for the butyl, hexyl, and octyl polymers: T_g essentially leveled off. The third- and fourth-generation polymers exhibited behavior resembling that of the second-generation polymer, with T_g decreasing and then leveling off with increasing alkyl chain length.

Polymer Morphology

Because the linear–dendritic rod diblock copolymers under investigation were also diblock copolymers, it was relevant to determine whether or not the two blocks would phase-segregate and assemble in the bulk and, if so, what kind of morphology would form and how the polymer assembly would be affected by the chemistry of the end groups, the generation number, and the architecture of the polymer. To do this, we used SAXS to determine whether or not periodic polymer domains formed and the sizes of the domains that formed; TEM was used to directly observe any existent phase-segregated domain morphology.

A TEM image of the room-temperature morphology of the PEO–LPEI diblock copolymer backbone is presented in Figure 10. Regions of weakly segregated polymer domains can be observed; overall, there is a lack of long-range order in the morphology. This lack of order was confirmed in the SAXS profiles, in which no strong scattering peaks were observed. This lack of long-range order was most likely due to the crystalline nature of each of the blocks, and this was consistent with the observations of Johnson et al.[79] for PEO–PAMAM hybrid linear–dendritic diblock copolymers. For the third-generation polymer, below 50 °C, the PEO block was crystalline, with no apparent phase segregation as the formation of the PEO crystals destroyed the morphology. However, above 50 °C, a segregated melt state formed with the melting of the PEO block. Similarly, Quiram et al.[80] reported that crystallization of the ethylene block in polyethylene–poly(3-methyl-1-butene) diblock copolymers completely disrupted the morphology when the blocks were weakly segregated. Given that both the PEO and PEI blocks in the PEO–LPEI diblock copolymer were crystalline, long-range order was most likely inhibited by the two competing crystalline states.

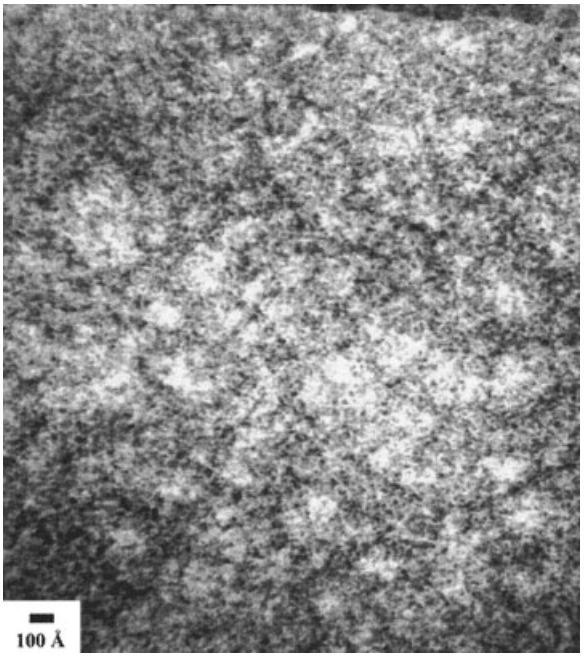

Figure 10. TEM image of the bulk morphology of the PEO–PEI diblock copolymer backbone at room temperature. The PEI block is stained.

Similarly, long-range order was not observed for the PEO–LPEI generation 0.5 linear–dendritic rod diblock copolymers. A TEM image of the polymer's room-temperature morphology is presented in Figure 11; the weight fraction of the dendritic block in the linear–dendritic rod diblock copolymer was 0.87. The dark, stained dendritic block regions appear to form irregularly shaped spheres and oblong domains within a continuous PEO matrix, even though the relatively high weight fraction of the dendritic block versus the PEO block would indicate a PEI–PAMAM continuous phase in a typical linear block copolymer. The morphology may be partially influenced by the solvent choice of methanol used in the preparation of the film; methanol may preferentially solvate the PEO domains in this case, this resulting in the formation of the PEO matrix. This weak, noncorrelated phase segregation results in diffuse scattering peaks observed in SAXS, and this indicates the absence of a long-range order, similar to the original LPEI–PEO block copolymer.

A disordered morphology was also observed in higher generations of the block copolymer series, as indicated by TEM and SAXS of the generation 4.5 PEO–LPEI PAMAM linear–dendritic rod diblock copolymer. It appears that the two blocks

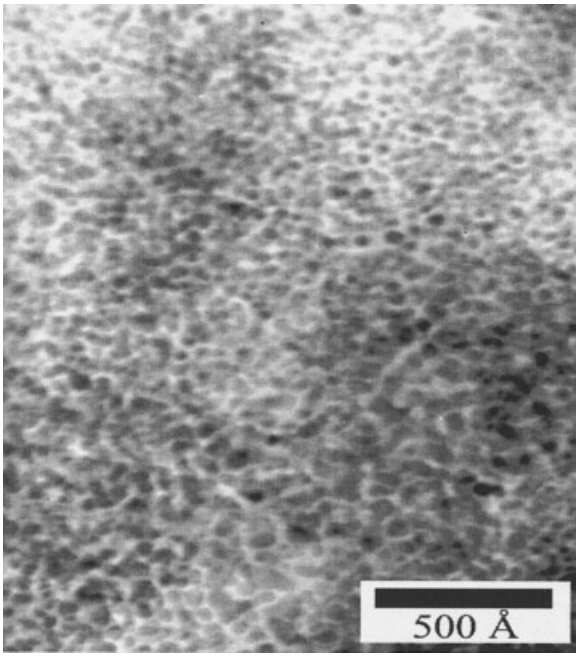

Figure 11. TEM image of the bulk morphology of the PEO–PEI generation 0.5 linear–dendritic rod diblock copolymer at room temperature. The dendritic portion is stained.

were not chemically incompatible enough to induce strong segregation, regardless of the presence of crystallinity in the PEO block. The morphology shown in Figure 12 looks remarkably similar to the disordered phase-segregated morphologies reported for generation 5 and 6 benzyl ether/polystyrene block copolymers. Mackay et al.[34] observed disordered morphologies at a high dendrimer weight fraction (67%), and ordered lamellar or cylindrical morphologies were observed at longer polystyrene chain lengths. Pochan et al.[36] found disordered morphologies at dendrimer fractions of 12% and lower. It is likely that at the high weight fractions of the dendrimer in these systems, with the moderate compatibility between the PEO and PAMAM blocks, phase segregation was weak throughout the range of generations observed here; much larger chain lengths of PEO may lead to stronger segregation in these systems. As the percentage of PEO decreased dramatically in generations 1.0 and higher, the tendency toward segregation greatly decreased. The morphology observed in these systems was a fine, bicontinuous morphology consisting of domains 2–5 nm long, as shown in Figure 12, and it is actually reminiscent of that observed for other comb polymer systems.[81]

The morphology of the dodecyl-terminated linear–dendritic rod diblock copolymers was also examined to determine the effect of adding alkyl groups to the polymer morphology. For the generation 1.0, 2.0, and 3.0 dodecyl polymers, no long-range order was detected by SAXS and TEM; TEM indicated a morphology very similar to that observed for the generation 4.5 polymer.

The only polymer that exhibited a predominate morphology was the PEO–PEI generation 4.0 dodecyl linear–dendritic rod diblock copolymer. A one-dimensional (1D) temperature-dependent SAXS profile and a TEM image of its room-temperature morphology are presented in Figures 13 and 14(a), respectively. From the SAXS profiles, a strong scattering peak was observed at room temperature that corresponded to a d-spacing of approximately 4.1 nm. This scattering peak decreased in intensity and eventually disappeared with increasing temperature because of melting of the alkyl chains, which were driving the phase segregation. A loss of the scattering peak occurred between 24 and 34 °C, which corresponded to T_m of the alkyl chains, as determined by DSC. As the scattering peak decreased in intensity with in-

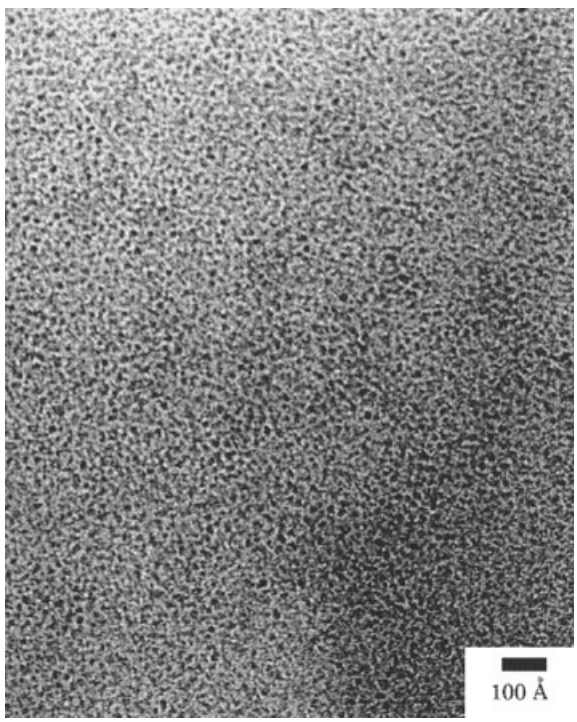

Figure 12. TEM image of the bulk morphology of the PEO–PEI generation 4.5 linear–dendritic rod diblock copolymer at room temperature. The dendritic portion is stained.

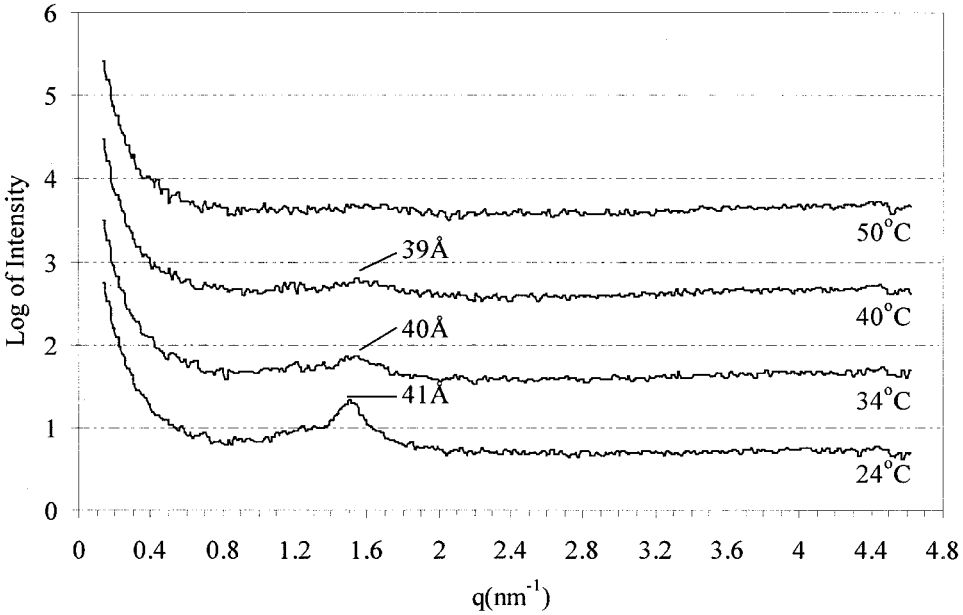

Figure 13. Temperature-dependent 1D SAXS profiles for the PEO–PEI generation 4.0 dodecyl-terminated linear–dendritic rod diblock copolymer.

creasing temperature, it also shifted to slightly smaller *d*-spacings: the shift was from 4.1 to 3.9 nm. These results were consistent with the TEM images of the polymer, which revealed a room-temperature morphology consisting of a supramolecular globular structure within which fine alternating dark and light domains were visible, resulting in a fingerprint-like image. In these images, the PAMAM portion was stained dark, whereas the alkyl chains and the PEO block appeared light. The value of the *d*-spacing determined for the fingerprint pattern within the dark globular domains was consistent with what might be expected for the diameter of an individual dendritic rod, and the width of the larger globular supramolecular domains was approximately the length expected for a dendritic rod. Thus, it appears as if the individual polymers were taking on a wormlike or rodlike ordered configuration. Figure 14(b) depicts a schematic model of possible arrangements of the dodecyl-substituted dendritic rod copolymer. On the basis of the bond lengths and angles, the length of an all-trans dodecyl chain was expected to be approximately 1.0–1.1 nm, leaving a 2.1-nm diameter for the PAMAM interior. This value was in good agreement with the diameter measured by Tomalia et al.[11] for the generation 4.5 PAMAM dendritic rod homopolymers terminated with sodium carboxylate groups. Using TEM, they measured a dendritic rod diameter of 2.5–3.2 nm for a polymer that was a full generation larger than the PAMAM interior in these dodecyl-terminated diblock copolymers. The shift in the *d*-spacing for the linear–dendritic rod diblock copolymers was most likely due to the melting of the crystalline alkyl chains into a less extended conformation. In addition, from the TEM images of the linear–dendritic rod diblock copolymers, the dark and light regions within the larger, darker, globular domains appeared to have approximately the same dimensions, in good agreement with the model proposed for the dimensions of these diblock copolymers. Nonetheless, if the PAMAM interior had adopted an all-trans conformation, the diameter of the interior would have been approximately 5.8 nm. Given that the measured diameter was much less than one for an all-trans configuration, it appears as if the PAMAM interior adopted a much more compact state, possibly because of incompatibility with the exterior alkyl chains. Overall, it appears as if the individual wormlike polymers were assembling into domains with the alkyl chains on adjacent polymers meeting end to end, as indicated in Figure 14(b). The nonuniformity of the film was likely enhanced by a lack of cohesion between PEO domains, and this may have resulted in the formation of the aggregate structures and discontinuous nature of the film.

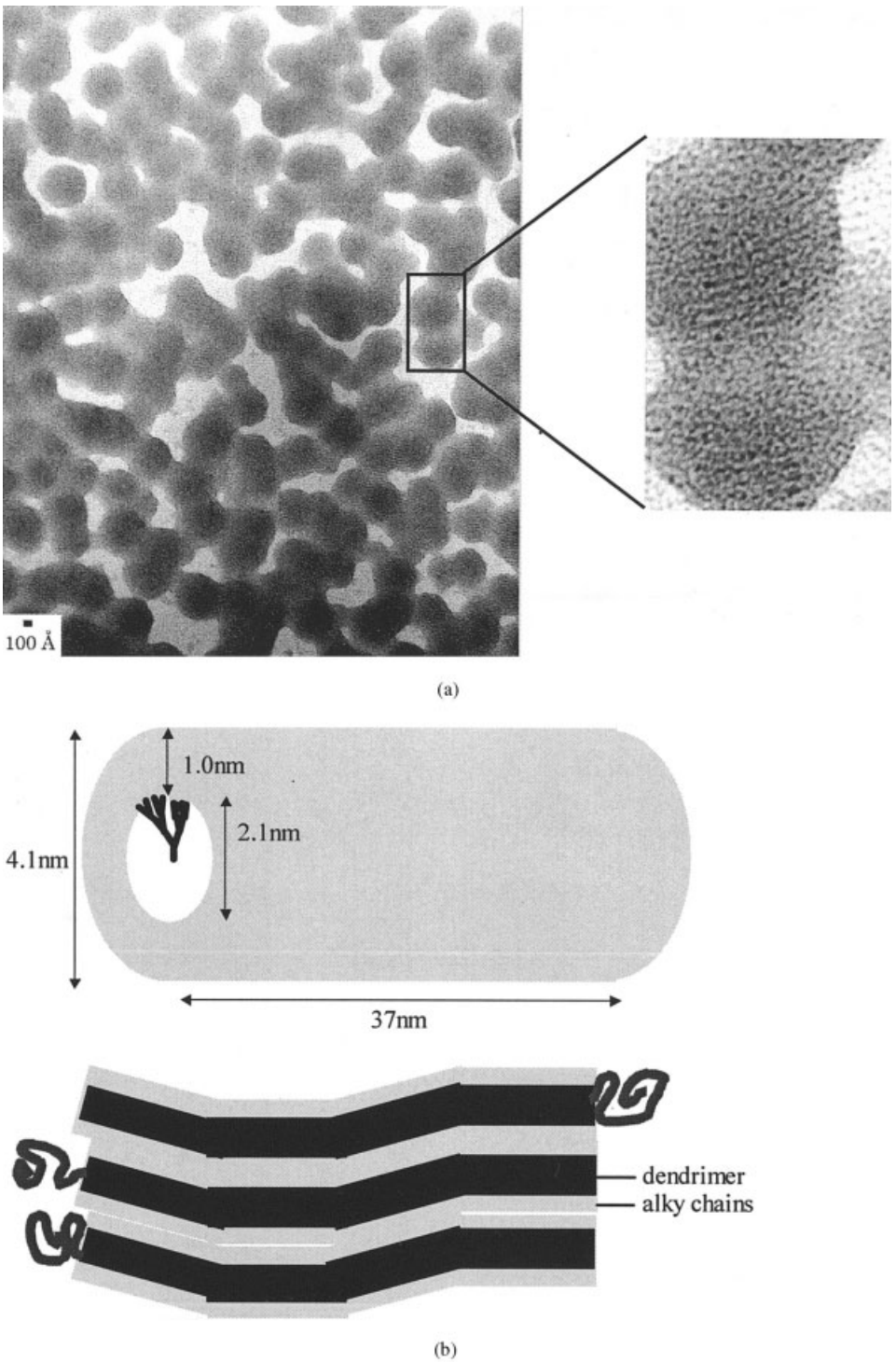

Figure 14. (a) TEM image of the bulk morphology of the PEO–PEI generation 4.0 dodecyl-terminated linear–dendritic rod diblock copolymer at room temperature (the PAMAM portion is stained) and (b) possible dimensions and arrangement of the PEO–PEI generation 4.0 dodecyl-terminated linear–dendritic rod diblock copolymers in the bulk.

These results are somewhat in contrast to those observed for hybrid linear–dendritic diblock copolymers reported by Johnson et al.[79] For the PEO–PAMAM hybrid linear–dendritic diblock copolymers, the morphology was strongly enhanced by the crystallinity of the alkyl chains for all the polymer generations examined, and this resulted in well-defined continuous lamellar domains. The novel architecture of the linear–dendritic rod diblock copolymers most likely contributed to the differences in the observations between the bulk morphologies of the linear–dendritic rod diblock copolymers and the hybrid linear–dendritic diblock copolymers. First, because the linear block in the linear–dendritic rod diblock copolymers was a much smaller component, it was not able to drive the segregation of the polymers to nearly the same extent as it had in the hybrid linear–dendritic diblock copolymers that possessed the same chemistry but a different architecture; thus, the morphologies of the linear–dendritic rod diblock copolymers were driven instead by the behavior of the dendritic block. Second, because the dendritic block in the linear–dendritic rod diblock copolymers did not assume its desired rodlike shape until the fourth generation, it was difficult for the shape and size of the polymer to drive the morphology as it had done in the polystyrene–poly(propylene imine) hybrid linear–dendritic diblock copolymers. Nonetheless, the shape and size of the dendritic rod block did become more defined as the generation number increased, and the resulting morphology of the diblock copolymer became more defined as well, in contrast to the observation for the polystyrene–poly(propylene imine) dendrimers, the morphology of which became less ordered as the generation increased.

CONCLUSIONS

Here we have reported the first synthesis of a new dendritic architecture—the linear–dendritic rod diblock copolymer—as well as an examination of the thermal and morphological properties of these novel polymers. These polymers were interesting because they possessed not only the unusual shape of the dendritic rod but also a linear block that added physical integrity and a driving force for the assembly of these polymers in solution, at the air–water interface, and in the bulk, when the chemistry of the polymers was properly tuned. Specifically, these linear–dendritic rod diblock copolymers consisted of a PEO–LPEI diblock copolymer backbone to which PAMAM branches were divergently synthesized around the PEI block.

The thermal and morphological properties of the polymers were examined with DSC, SAXS, and TEM. Both the dendritic and diblock copolymer nature of the polymer were reflected in the thermal behavior of the polymers. As observed for spherical dendrimers and hybrid linear–dendritic diblock copolymers, T_g of the dendritic block was highly dependent on the chemistry of the branch ends. Furthermore, T_g of the dendritic block increased with increasing generation, most likely because of the increased stiffness of the branches and the increased dispersive forces between the dendrimers.

For most of the polymers, a weakly phase-segregated morphology typical of comb copolymers was observed. Although the TEM images of the polymers revealed phase segregation, no long-range order was observed, and this was consistent with the absence of scattering peaks in SAXS. When, however, the generation 3.5 block copolymer was substituted with long dodecyl alkyl chains, a well-defined and ordered morphology was observed, suggesting that strong phase segregation was possible in larger, higher molecular weight block copolymer systems. This polymer exhibited a strong SAXS scattering peak at a *d*-spacing of 4.1 nm. TEM images of this polymer revealed a wormlike or rodlike morphology: the diameter of the worms was approximately 4 nm, and the length was approximately 30–40 nm. These dimensions were consistent with those of an individual polymer, and this indicated that the generation 4.0 dodecyl polymers adopted a wormlike or rodlike conformation.

The authors thank the Environmental Protection Agency (Young Investigator Award STAR Grant R825224-01-0), the National Science Foundation Division of Materials Research (Creativity Extension DMR-9903380), and the 3M Innovation Fund for funding. They also thank Mitch Anthamatten for his assistance with the small-angle X-ray scattering experiments; Kris Stokes for his creation of the cover graphics and figure modification; Peter Dvornic, Peter Carver, and Tom Chamberlin of the Michigan Molecular Institute/Impact Analytical for performing gel permeation chromatography/light scattering experiments; and Anne Mayes for helpful discussions. Finally, the authors thank the Massachusetts Institute of Technology MRSEC Program of the National Science Foundation (DMR 02-13282) for the use of the CMSE facilities.

REFERENCES AND NOTES

1. Fréchet, J. M. J. J Polym Sci Part A: Polym Chem 2003, 41, 3713–3725.
2. Percec, V.; Cho, W. D.; Ungar, G.; Yeardley, D. J. P. Angew Chem Int Ed 2000, 39, 1598.
3. Tomalia, D. A.; Fréchet, J. M. J. J Polym Sci Part A: Polym Chem 2002, 40, 2719–2728.
4. Tully, D. C.; Fréchet, J. M. J. Chem Commun 2001, 1229–1239.
5. Hawker, C. J.; Fréchet, J. M. J. Polymer 1992, 33, 1507–1511.
6. Tomalia, D. A.; Durst, H. D. Top Curr Chem 1994, 165, 193–313.
7. Hobson, L. J.; Kenwright, A. M.; Feast, W. J. Chem Commun 1997, 1877–1878.
8. Merino, S.; Brauge, L.; Caminade, A. M.; Majoral, J. P.; Taton, D.; Gnanou, Y. Chem—Eur J 2001, 7, 3095–3105.
9. Guan, Z. J Polym Sci Part A: Polym Chem 2003, 41, 3680–3692.
10. Knauss, D. M.; Al-Muallem, H. A.; Huang, T. Z.; Wu, D. T. Macromolecules 2000, 33, 3557–3568.
11. Yin, R.; Zhu, Y.; Tomalia, D. A.; Ibuki, H. J Am Chem Soc 1998, 120, 2678–2679.
12. Percec, V.; Ahn, C. H.; Cho, W. D.; Jamieson, A. M.; Kim, J.; Leman, T.; Schmidt, M.; Gerle, M.; Moller, M.; Prokhorova, S. A.; Sheiko, S. S.; Cheng, S. Z. D.; Zhang, A.; Ungar, G.; Yeardley, D. J. P. J Am Chem Soc 1998, 120, 8619–8631.
13. Percec, V.; Ahn, C. H.; Ungar, G.; Yeardley, D. J. P.; Moller, M.; Sheiko, S. S. Nature 1998, 391, 161–164.
14. Percec, V.; Cho, W. D.; Mosier, P. E.; Ungar, G.; Yeardley, D. J. P. J Am Chem Soc 1998, 120, 11061–11070.
15. Percec, V.; Holerca, M. N.; Magonov, S. N.; Yeardley, D. J. P.; Ungar, G.; Duan, H.; Hudson, S. D. Biomacromolecules 2001, 2, 706–728.
16. Neubert, I.; Amoulong-kirstein, E.; Schluter, A. D.; Dautzenberg, H. Macromol Rapid Commun 1996, 17, 517–527.
17. Neubert, I.; Schluter, A. D. Macromolecules 1998, 31, 9372–9378.
18. Stocker, W.; Schurmann, B. L.; Rabe, J. P.; Forster, S.; Lindner, P.; Neubert, I.; Schluter, A. D. Adv Mater 1998, 10, 793–797.
19. Shu, L. J.; Schluter, A. D.; Ecker, C.; Severin, N.; Rabe, J. P. Angew Chem Int Ed 2001, 40, 4666.
20. Ouali, N.; Mery, S.; Skoulios, A.; Noirez, L. Macromolecules 2000, 33, 6185–6193.
21. Gitsov, I.; Wooley, K. L.; Hawker, C. J.; Ivanova, P. T.; Frechet, J. M. J. Macromolecules 1993, 26, 5621–5627.
22. Gitsov, I.; Fréchet, J. M. J. Macromolecules 1994, 27, 7309–7315.
23. Gitsov, I.; Lambrych, K. R.; Remnant, V. A.; Pracitto, R. J Polym Sci Part A: Polym Chem 2000, 38, 2711–2727.
24. Gitsov, I.; Wooley, K. L.; Fréchet, J. M. J. Angew Chem Int Ed Engl 1992, 31, 1200–1202.
25. van Hest, J. C. M.; Delnoye, D. A. P.; Baars, M.; Elissen-Román, C.; van Genderen, M. H. P.; Meijer, E. W. Chem—Eur J 1996, 2, 1616–1626.
26. van Hest, J. C. M.; Delnoye, D. A. P.; Baars, M.; van Genderen, M. H. P.; Meijer, E. W. Science 1995, 268, 1592–1595.
27. van Hest, J. C. M.; Baars, M.; Elissen-Román, C.; van Genderen, M. H. P.; Meijer, E. W. Macromolecules 1995, 28, 6689–6691.
28. Roman, C.; Fischer, H. R.; Meijer, E. W. Macromolecules 1999, 32, 5525–5531.
29. Chang, Y.; Kwon, Y. C.; Lee, S. C.; Kim, C. Macromolecules 2000, 33, 4496–4500.
30. Chang, Y. Y.; Kim, C. J Polym Sci Part A: Polym Chem 2001, 39, 918–926.
31. Chapman, T. M.; Hillyer, G. L.; Mahan, E. J.; Shaffer, K. A. J Am Chem Soc 1994, 116, 11195–11196.
32. Iyer, J.; Fleming, K.; Hammond, P. T. Macromolecules 1998, 31, 8757–8765.
33. Leduc, M. R.; Hawker, C. J.; Dao, J.; Fréchet, J. M. J. J Am Chem Soc 1996, 118, 11111–11118.
34. Mackay, M. E.; Hong, Y.; Jeong, M.; Tande, B. M.; Wagner, N. J.; Hong, S.; Gido, S. P.; Vestberg, R.; Hawker, C. J. Macromolecules 2002, 35, 8391–8399.
35. Tande, B. M.; Wagner, N. J.; Mackay, M. E. C R Chim 2003, 6, 853–864.
36. Pochan, D. J.; Pakstis, L.; Huang, E.; Hawker, C. J.; Vestberg, R.; Pople, J. Macromolecules 2002, 35, 9239–9242.
37. Aoi, K.; Motoda, A.; Ohno, M.; Tsutsumiuchi, K.; Okada, M.; Imae, T. Polym J 1999, 31, 1071–1078.
38. Al-Muallem, H. A.; Knauss, D. M. J Polym Sci Part A: Polym Chem 2001, 39, 152–161.
39. Iyer, J.; Hammond, P. T. Langmuir 1999, 15, 1299–1306.
40. Johnson, M. A.; Santini, C. M. B.; Iyer, J.; Satija, S.; Ivkov, R.; Hammond, P. T. Macromolecules 2002, 35, 231–238.
41. Imae, T.; Ito, M.; Aoi, K.; Tsutsumiuchi, K.; Noda, H.; Okada, M. Colloids Surf A 2000, 175, 225–234.
42. Stupp, S. I.; LeBonheur, V.; Walker, K.; Li, L. S.; Huggins, K. E.; Keser, M.; Amstutz, A. Science 1997, 276, 384–389.
43. Zubarev, E. R.; Pralle, M. U.; Li, L. M.; Stupp, S. I. Science 1999, 283, 523–526.
44. Lecommandoux, S.; Klok, H. A.; Sayar, M.; Stupp, S. I. J Polym Sci Part A: Polym Chem 2003, 41, 3501–3518.
45. Gopalan, P.; Li, X.; Li, M.; Ober, C. K.; Gonzalez, C. P.; Hawker, C. J. J Polym Sci Part A: Polym Chem 2003, 40, 3640–3656.
46. Radzilowski, L. H.; Carragher, B. O. Macromolecules 1997, 30, 2110–2119.

47. Chen, J. T.; Thomas, E. L.; Ober, C. K.; Hwang, S. S. Macromolecules 1995, 28, 1688–1697.
48. Zubarev, E. R.; Stupp, S. I. J Am Chem Soc 2002, 124, 5762.
49. Fischer, P.; Brooks, C. F.; Fuller, G. G.; Ritcey, A. M.; Xiao, Y. F.; Rahem, T. Langmuir 2000, 16, 726–734.
50. Armarego, W. L. F.; Perrin, D. D. Purification of Laboratory Chemicals, 4th ed.; Butterworth-Heinemann: Oxford, 1997; p 343.
51. Dust, J. M.; Fang, Z. H.; Harris, J. M. Macromolecules 1990, 23, 3742–3746.
52. Overberger, C. G.; Peng, L. J Polym Sci Part A: Polym Chem 1986, 24, 2797–2813.
53. Tomalia, D. A.; Baker, H.; Dewald, J.; Hall, M.; Kallos, G.; Martin, S.; Roeck, J.; Ryder, J.; Smith, P. Polym J 1985, 17, 117–132.
54. Tomalia, D. A.; Baker, H.; Dewald, J.; Hall, M.; Kallos, G.; Martin, S.; Roeck, J.; Ryder, J.; Smith, P. Macromolecules 1986, 19, 2466–2468.
55. Vandermiers, C.; Damman, P.; Dosiere, M. Polymer 1998, 39, 5627–5631.
56. Miyamoto, M.; Sano, Y.; Saegusa, T.; Kobayashi, S. Eur Polym J 1983, 19, 955–961.
57. Simionescu, C. I.; Rabia, I. Polym Bull 1983, 10, 311–314.
58. Maechling-Strasser, C.; Dejardin, P.; Galin, J. C.; Schmitt, A.; Housseferrari, V.; Sebille, B.; Mulvihill, J. N.; Cazenave, J. P. J Biomed Mater Res 1989, 23, 1395–1410.
59. Saegusa, T.; Ikeda, H.; Fujii, H. Macromolecules 1972, 5, 108.
60. Liu, Q.; Konas, M.; Riffle, J. S. Macromolecules 1993, 26, 5572–5576.
61. Liu, Q.; Wilson, G. R.; Davis, R. M.; Riffle, J. S. Polymer 1993, 34, 3030–3036.
62. Wyatt, P. Anal Chim Acta 1993, 272, 1.
63. Johann, C.; Kilz, P. J Appl Polym Sci Appl Polym Symp 1991, 48, 111.
64. Gerle, M.; Fischer, K.; Roos, S.; Muller, A. H. E.; Schmidt, M.; Sheiko, S. S.; Prokhorova, S.; Moller, M. Macromolecules 1999, 32, 2629–2637.
65. Saegusa, T.; Fujii, H.; Ikeda, H. U.S. Patent 3,821,125, 1974.
66. Goethals, E. J. In Ring Opening Polymerization; Ivin, K. J.; Saegusa, T., Eds.; Elsevier: Amsterdam, 1984; Vol. 2, pp 715–807.
67. Brandrup, J.; Immergut, E. H. Polymer Handbook, 3rd ed.; Wiley: New York, 1989.
68. Weyts, K. F.; Goethals, E. J. Polym Bull 1988, 19, 13–19.
69. Wooley, K. L.; Hawker, C. J.; Pochan, J. M.; Fréchet, J. M. J. Macromolecules 1993, 26, 1514–1519.
70. de Brabander-van de Berg, E. M. M.; Meijer, E. W. Angew Chem Int Ed Engl 1993, 32, 1308–1311.
71. Malmstrom, E.; Hult, A.; Gedde, U. W.; Liu, F.; Boyd, R. H. Polymer 1997, 38, 4873–4879.
72. Stutz, H. J Polym Sci Part B: Polym Phys 1995, 33, 333–340.
73. Dvornic, P. R.; de Leuze-Jallouli, A. M.; Owen, M. J.; Perz, S. V. Macromolecules 2000, 33, 5366–5378.
74. Mogri, Z.; Paul, D. R. Polymer 2001, 42, 7765–7780.
75. Wei, H. Y.; Shi, W. F.; Nie, K. M.; Shen, X. F. Polymer 2002, 43, 1969–1972.
76. Malmstrom, E.; Johansson, M.; Hult, A. Macromol Chem Phys 1996, 197, 3199–3207.
77. Wu, F. I.; Shu, C. F. J Polym Sci Part A: Polym Chem 2001, 39, 2536–2546.
78. Mogri, Z.; Paul, D. R. J Membr Sci 2000, 175, 253–265.
79. Johnson, M. A.; Iyer, J.; Hammond, P. T. Macromolecules, in press.
80. Quiram, D. J.; Register, R. A.; Marchand, G. R.; Ryan, A. J. Macromolecules 1997, 30, 8338–8343.
81. Mayes, A. Massachusetts Institute of Technology, Cambridge, MA. Personal communication, 2002.